Effects of nitrate and phosphate supply on chromophoric and fluorescent dissolved organic matter in the Eastern Tropical North Atlantic: a mesocosm study

A.N. Loginova*[1], C. Borchard[1], J. Meyer[1], H. Hauss[1], R. Kiko[1], and A. Engel[1]

[1]GEOMAR Helmholtz-Centre for Ocean Research Kiel, Düsternbrooker Weg 20, 24105 Kiel, Germany

*Correspondence should be addressed to: aloginova@geomar.de

Key words: Dissolved Organic Carbon (DOC), humic-like fluorescence, tyrosine-like fluorescence, tryptophan-like fluorescence

Abstract

In open ocean regions, as is the Eastern Tropical North Atlantic (ETNA), pelagic production is the main source of dissolved organic matter (DOM) and is affected by dissolved inorganic nitrogen (DIN) and phosphorus (DIP) concentrations. Changes in pelagic production under nutrient amendments were shown to also modify DOM quantity and quality. However, little information is available about the effects of nutrient variability on chromophoric (CDOM) and fluorescent (FDOM) DOM dynamics. Here we present results from two mesocosm experiments ("Varied P" and "Varied N") conducted with a natural plankton community from the ETNA, where the effects of DIP and DIN supply on DOM optical properties were studied. CDOM accumulated proportionally to phytoplankton biomass during the experiments. Spectral slope (*S*) decreased over time indicating accumulation of high molecular weight DOM. In Varied N, an additional CDOM portion, as a result of bacterial DOM reworking, was determined. It increased the CDOM fraction in DOC proportionally to the supplied DIN. The humic-like FDOM component (Comp.1) was produced by bacteria proportionally to DIN supply. The protein-like FDOM component (Comp.2) was released irrespectively to phytoplankton or bacterial biomass, but depending on DIP and DIN concentrations. Under high DIN supply, Comp.2 was removed by bacterial reworking, leading to an accumulation of humic-like Comp.1. No influence of nutrient availability on amino acid-like FDOM component in peptide form (Comp.3) was observed. Comp.3 potentially acted as an intermediate product during formation or degradation Comp.2. Our findings suggest that changes in nutrient concentrations may lead to substantial responses in the quantity and quality of optically active DOM and, therefore, might bias results of the applied *in situ* optical techniques of DOC estimations concentrations in open ocean regions.

Introduction

Dissolved organic matter (DOM) is the largest dynamic pool of organic carbon in the ocean. Its global inventory constitutes of approximately 662 pentagrams of carbon (PgC) (Hansell et al., 2009). Labile and semi-labile high molecular weight (HMW) DOM is released primarily by phytoplankton (Carlson and Hansell, 2015). It is used as substrate by heterotrophic communities, which, in turn, release less bioavailable semi-refractory or even refractory DOM, thereby modifying the quantity and quality of the DOM pool (Azam et al., 1983, Ogawa et al., 2001, Jiao et al., 2010). Therefore, natural DOM is a complex mixture of organic compounds with different characteristics, such as molecular structure and molecular weight, resulting in different optical properties (Stedmon and Nelson, 2015).

For instance, the presence of conjugated double bonds (polyenes) results in the absorption of light in the UV and visible wavelengths (Stedmon and Álvarez-Salgado, 2011). The light absorbing DOM fraction is referred to as 'chromophoric' or 'colored' DOM (CDOM) (Coble, 2007). Due to its abilities to absorb in a wide wavelength range, CDOM may protect primary producers from harmful UV irradiation in the water column, but may also reduce photosyntetically active radiation, as it absorbs at similar wavelength as the first chlorophyll absorption maximum (~443 nm) (Zepp et al., 2008). Photons, absorbed by CDOM, may induce the formation of free radicals, which by colliding with other molecules or other radicals produce new organic molecules, reducing metals or introducing short inorganic and organic substances as byproducts (Sulzberger and Durisch-Kaiser, 2008). Modified by photoreactions, CDOM may serve, as biological substrates for auto- and heterotrophic communities, by releasing nutrients and low molecular weight (LMW) organic compounds, as well as a source of trace gases (e.g. CO, CO_2) (Kieber et al., 1990, Moran and Zepp, 1997, Kieber et al., 1999).

CDOM absorption has often been used as an indicator for dissolved organic carbon (DOC) concentrations in the Ocean (Fichot and Benner, 2011, 2012, Rochelle-Newall et al., 2014). For example, DOC concentration in estuarine surface waters can be derived from CDOM absorption by remote sensing techniques, assuming a direct relationship between CDOM absorption and DOC concentrations (Del Castillo, 2005, 2007). In the open ocean, however, this relationship varies throughout the water column (Nelson and Siegel, 2013), and factors affecting it are poorly understood.

A better knowledge on factors influencing the CDOM/DOC relationship could improve our understanding of DOM cycling, as well as of the regulation of light attenuation in the ocean.

Furthermore, the knowledge of the factors, influencing the open ocean CDOM/DOC relationship would be useful for the estimation of DOC concentrations from CDOM absorption measurements by remote sensing techniques.

As CDOM embodies a complex mixture of organic compounds that have overlapping absorption spectra, with, generally, no single compound dominating (Del Vecchio and Blough, 2004), CDOM absorbance spectra decrease exponentially toward longer wavelength, with no discernible peaks. Therefore, the CDOM concentration is commonly expressed as absorption coefficient at chosen wavelength (e.g. 325, 355, 375nm) (Stedmon and Markager, 2001, Fichot and Benner, 2012, Nelson and Siegel, 2013).

To derive information on CDOM quality, such as molecular weight and modification processes, spectral slopes (S) of CDOM light absorption and spectral slopes ratio (S_R) are used (Helms et al., 2008, Zhang et al., 2009). It has been shown that S decrease with increasing DOM molecular weight, and, therefore, may be used as an indicator of accumulation/degradation of bioavailable HMW-DOM (De Haan and De Boer, 1987, Helms et al., 2008, Zhang et al., 2009).

The ratio of S at wavelength region 275-295 nm ($S_{275\text{-}295}$) to S at 350-400 nm ($S_{350\text{-}400}$), S_R, is used to estimate CDOM transformation processes. S_R increases as CDOM becomes involved in photoreactions and decreases as CDOM undergoes microbial reworking (Helms et al., 2008).

The presence of aromatic rings in CDOM often also results in fluorescence (Stedmon and Álvarez-Salgado, 2011). Fluorescent DOM (FDOM) excitation/emission (Ex/Em) spectra allow discriminating between different pools of CDOM (Coble, 2007, Stedmon and Bro, 2008, Mopper et al., 2007, Yamashita et al., 2010). The substances that are excited and emit in the UV spectral range commonly correspond to labile proteinaceous DOM, and therefore are referred to as amino acid-like (tyrosine- and tryptophan-like) FDOM (e.g. Coble, 1996). The substances that are excited in the UV spectral range, but emit in the visible spectral range were identified as fulvic- and humic-like FDOM (Gueguen and Kowalczuk, 2013). Tyrosine- and Tryptophan-like substances have been used for the assessment of *in situ* primary productivity, while humic-like substances are used for the indication of allochtonous (e.g. riverine) DOM or microbial DOM transformation (Coble, 1996).

Although the CDOM and FDOM distribution and cycling has been described for many open ocean sites (Jørgensen et al., 2011, Kowalczuk et al., 2013, Nelson and Siegel, 2013), specific sources and factors influencing their composition and transformations are yet not well understood.

For example, CDOM accumulation is often related to nutrient remineralization (Swan et al., 2009, Nelson and Siegel, 2013). However, the effects of nutrient variability on CDOM concentration and on the relationship between CDOM and DOC are largely understudied.

Stedmon and Markager (2005) have reported that nutrients affect freshly produced marine FDOM pools in temperate climate conditions (Raunefjord, Norway). In their study, the amino acid-like fluorescence was enhanced under phosphate (P) and silica limitation, but was independent from phytoplankton composition. Bacterially produced humic-like FDOM components were reported to accumulate under P and silica limitation as well. Later, by addition of different synthetic dissolved organic and inorganic nitrogen (N) substrates to microbial incubations, Biers et al. (2007) emphasized the role of N in CDOM accumulation. They showed that CDOM and FDOM production by bacteria, cultured in natural seawater medium, can be affected to different degrees by the chemical composition and steric effects of the organic N source, while inorganic N sources do not contribute significantly to CDOM or FDOM accumulation. On the other hand, Kramer and Herndl (2004) demonstrated that bacteria may be able to transform about 30% of taken up inorganic N into semi-labile to refractory humic DOM.

Stedmon and Markager (2005), however, revealed some doubts about a setup of P limitation. Besides, Kramer and Herndl (2004) and Biers et al. (2007) were based on single bacterial cultures, and phytoplankton and net-effects, associated with natural aquatic bacterial community, were excluded. Therefore, the influence of inorganic nutrients on CDOM concentration and FDOM components in natural waters remains to be resolved.

In the open ocean regions, as is the Eastern Tropical North Atlantic (ETNA), pelagic production of DOM is, supposedly, of greater importance than terrestrial DOM input (e.g. Coble et al., 2007).

In classical view, the ETNA is considered an "excess N" region compared to the 'Redfield N:P ratio' of 16 (see Redfield, 1987 and Gruber and Sarmento, 1997) reflecting high rates of biological N-fixation due to Saharan dust deposition, with N:P ratios 16-25 at depth (see Fanning, 1992). It features a shallow Oxygen Minimum Zone (OMZ) at about 100 m depth with oxygen concentrations about 60 µmol O_2 kg^{-1} (Brandt et al., 2015) and a deeper OMZ at approximately 300-600 m depth with oxygen concentrations up to 40 O_2 µmol kg^{-1} (Karstensen et al., 2008). However, eddies originating in the Mauritanian upwelling regime and propagating westward can harbor much lower oxygen concentrations (~4 µmol O_2 kg^{-1}; Karstensen et al., 2014), potentially enabling N-loss processes (Strous et al., 2006, Kartal et

al., 2007, Jetten et al., 2009, Jayakumar et al., 2009). Those mesoscale eddies, may transport nutrient loaded but relatively N deficient waters to the surface (McGillicudy et al., 2003, 2007, Mathis et al., 2007). Furthermore, it has been shown that non-diazotroph primary production in the surface waters of ETNA can be N-limited (Franz et al., 2012, Hauss et al., 2013).

Here we investigated the effects of different dissolved inorganic nitrogen (DIN) and dissolved inorganic phosphorous (DIP) concentrations and of their supply ratio (DIN:DIP) on DOM quantity and quality by using spectroscopic methods of DOM analysis (e.g. accumulation and properties of CDOM and FDOM) during mesocosm study with natural pelagic community off the Cape Verdean Archipelago, an area, affected by low oxygen-core eddies.

During these mesocosm experiments, we tested whether (1) pelagic production is a source of CDOM and FDOM, (2) CDOM and FDOM accumulation and composition are affected by changes in nutrient stoichiometry, and whether (3) the relationship between CDOM absorption and DOC concentrations is stable under variable nutrient concentrations.

To do so, DOC concentrations, CDOM absorption and CDOM spectral properties ($S_{275\text{-}295}$ and S_R), FDOM fluorescence, as well as chlorophyll *a* (chl *a*), and bacterial abundance, were analyzed during the course of two mesocosm experiments, conducted as a part of the Collaborative Research Centre 754 (SFB754) "Climate-Biogeochemistry Interactions in the Tropical Ocean" (www.sfb754.de).

2. Methods

2.1 Setup of the mesocosms experiment

Two 8-day mesocosm experiments were conducted consecutively in October 2012 at the Instituto Nacional de Desenvolvimento das Pescas (INDP), Mindelo, Cape Verde. Seawater from 5 m depth was collected into four 600L tanks in the night of the 01.10/02.10 and 11.10/12.10 for the first and second experiment, respectively. The sampling was done with the RV *Islândia* south of São Vicente (16°44.4'N, 25°09.4'W). For each experiment, sixteen mesocosm-bags were placed floating in 4 'flow-through' cooling baths that were kept at surface seawater temperature (25.9 - 28.7°C) with the water from the Mindelo bay in front of the INDP. The mesocosms were filled alternately (about 10 seconds per filling event) and randomly from the tanks by gravity flow using submerged hose in order to achieve even distribution of the water and minimize bubble formation. A mesh to filter zooplankton was not used. The precise volume of each mesocosm was determined by addition of 1.5 mmol of silicate and subsequent measurement of the resulting silicate concentration. The water volume in the mesocosms ranged from 106 to 145L. For simulation of surface water conditions, the mesocosms were shaded with blue transparent lids to approximately 20% of sunlit irradiation (56-420 µE m^{-2} s^{-1}, depending on cloud cover).

Nutrients were manipulated by adding different amounts of phosphate (DIP) and nitrate (DIN). In the first experiment, the DIP supply was varied ("Varied P") at relatively constant DIN concentrations in twelve of the sixteen mesocosms, while in the second experiment the initial DIN concentrations were varied ("Varied N") at constant DIP supply in twelve of the sixteen mesocosms.

In addition to this, four 'cornerpoints', where both, DIN and DIP, were varied, were chosen to be repeated during both experiments (see target DIN and DIP values in Table 1). However, during the first experiment, setting the nutrient levels in one of the 'cornerpoint' mesocosms (mesocosm 10) was not successful and it was decided to adjust the DIN and DIP concentrations in this mesocosm to 'Redfield N:P ratio' of 16 (Redfield, 1987) and therefore add another replicate to the treatment 12.00N/0.75P. Another 'cornerpoint' mesocosm (mesocosm 5) during the first experiment was excluded from further analyses as no algal bloom had developed.

Initial sampling for biogeochemical parameters was accomplished immediately after the mesocosms filling (day 1). Nutrients were added after the initial sampling. Daily water sampling was conducted between 9:00 and 10:30 a.m. on days 2 to 8.

The target and actual nutrient concentrations are shown in Table 1 and the corresponding treatment indications will be used in the following.

2.2 Sampling and Analyses

2.2.1 Particulate organic matter

Samples of 500 mL for chl *a* measurements were vacuum-filtered (< 200 mbar) onto Whatman GF/F filters (25 mm, 0.7 µm), 1 ml of ultrapure water was added and the filters were frozen at -20°C for at least 24 hours. Subsequently, pigments were extracted using acetone and measured in a Trilogy® fluorometer (Turner Designs) calibrated with a chl *a* standard (*Anacystis nidulans*, Walter CMP, Kiel, Germany) dilution series (Parsons et al., 1984).

For bacterial cell counts, samples (5 mL) were fixed with 2% formaldehyde, frozen at -80°C and transported to the home laboratory. Samples were diluted 1:3, stained with SYBR-Green and measured at a flow rate of 11.0 µL min^{-1} by flow cytometry (FACScalibur, Becton Dickinson, San Jose, CA, USA).

2.2.3 Dissolved organic matter

Dissolved organic carbon (DOC) duplicate samples (20 mL) were filtered through combusted GF/F filters and collected in combusted glass ampoules. Samples were acidified with 80 µL of 85% phosphoric acid, flame sealed and stored at 4°C in the dark until analysis.

DOC samples were analysed by applying the high-temperature catalytic oxidation method (TOC -VCSH, Shimadzu) adapted from Sugimura and Suzuki (1998). The instrument was calibrated every 8-10 days by measuring of 6 standard solutions of 0, 500, 1000, 1500, 2500 and 5000 µgC L^{-1}, prepared using a potassium hydrogen phthalate standard (Merck 109017). Every day before each set of measurements, ultrapure (MilliQ) water was used for setting the instrument baseline, following by the measurement of the deep-sea water standard (Dennis Hansell, RSMAS, University of Miami) with known DOC concentration in order to verify result representation by the instrument. Additionally, two DOC control samples were prepared each day of measurement using a potassium hydrogen phthalate standard (Merck 109017). The control samples had dissolved carbon concentrations within the range of those in samples and were measured along the sample analyses in order to avoid mistakes due to baseline flow during measurements. The DOC concentration was determined in each sample out of 5 to 8 replicate injections.

For chromophoric dissolved organic matter (CDOM) and fluorescent dissolved organic matter (FDOM), duplicate samples of 35ml for each parameter were collected daily into combusted (450°C, 8 hours) amber-glass vials after filtering through 0.45 µm polyethersulfone syringe filters (CHROMAPHIL® Xtra PES-45/25, MACHEREY-NAGEL GmbH & Co.KG). The samples were stored at 4°C in the dark during 6 month pending analyses. All samples were brought to room temperature before analyses.

Absorption of chromophoric dissolved organic matter (CDOM) was detected using a 100 cm path length liquid waveguide cell (LWCC-2100, World Precision Instruments, Sarasota, Florida) and a UV-VIS spectrophotometer (Ocean Optics USB 4000) in conjunction with the Ocean Optics DT-MINI-CS light source. The absorbance was measured against ultrapure water (MilliQ) by injection to the cell with a peristaltic pump. The measurements were done over spectral range of 178.23 to 885.21 nm at 0.22 nm interval.

For the determination of fluorescent dissolved organic matter (FDOM), 3D fluorescence spectroscopy - Excitation-Emission Matrix Spectroscopy (EEMs) - was performed using a Cary Eclipse Fluorescence Spectrophotometer (Agilent Technologies) equipped with a xenon flash lamp. The fluorescence spectra for samples were measured in a 4-optical window 1 cm Quartz SUPRASIL® precision cell (Hellma®Analytics). The blank-3D fluorescence spectra and Water Raman scans were performed daily using an Ultra-Pure Water Standard sealed cuvette (3/Q/10/WATER; Starna Scientific Ltd). The experimental wavelength range for sample and ultra-pure water scans was 230 to 455 nm in 5 nm intervals on excitation and 290 to 700 nm in 2 nm intervals on emission. Water Raman scans were recorded from 285 to 450 nm at 1 nm intervals for emission at the 275 nm excitation wavelength (Murphy et al., 2013). All fluorescence measurements were managed at 19°C (Cary Single Cell Peltier Assessory, VARIAN), PMT 900V, 0.2 s integration times and 5 nm slit width on excitation and emission monochromators. The absorbance for EEMs corrections was procured simultaneously with Shimadzu® 1800 UV-VIS double-beam spectrophotometer. The absorbance was measured at the room temperature (~19°C) in 2-optical window 5 cm Quartz SUPRASIL® precision cell (Hellma®Analytics). The measurements were done at 1 nm wavelengths intervals from 230 to 750 nm against MilliQ water as a reference. The obtained data were converted to absorbance in a 1 cm cell.

2.3 Data evaluation

2.3.1 CDOM

The measured CDOM absorbance spectra were corrected to the refractive index of remaining particulate matter and colloids after Zhang et al. (2009) and for salinity after Nelson et al. (2007), and converted to absorption coefficients according to Bricaud et al. (1981):

$$a_{CDOM}(\lambda) = 2.303 \times A(\lambda)/L; \quad (1)$$

where $a_{CDOM}(\lambda)$ – is the absorption coefficient at wavelength λ (m^{-1}), $A(\lambda)$ - is the absorbance value at same wavelength and L – is the effective optical path length (m).

In in rivers and the coastal waters, absorption coefficients at 355 ($a_{CDOM}(355)$) and 375 ($a_{CDOM}(375)$) nm are commonly used to express CDOM concentrations (Granskog et al., 2007, Stedmon et al., 2011). Absorption coefficients at 440-445nm ($a_{CDOM}(440)$) are used for comparison of field CDOM measurements to remote sensing (Swan et al., 2013). In open ocean blue waters, absorbance at wavelengths of 400-600 nm is very low. Therefore, absorption at 325 nm ($a_{CDOM}(325)$) is often used for expression of the open ocean CDOM concentrations (Nelson and Siegel, 2013). The area off Cape Verdean Archipelago, where water for mesocosms was taken, is not influenced by river inflow and is considered as the open ocean area. Thus, $a_{CDOM}(325)$ was chosen for expression of CDOM concentration.

Spectral slopes for the intervals 275-295nm ($S_{275\text{-}295}$) and 350-400 ($S_{350\text{-}400}$) were calculated after Helms et al. (2008) using log-transform linear regression.

The CDOM alteration indicator, slope ratio (S_R), was also calculated after Helms et al. (2008) as well, as ratio of $S_{275\text{-}295}$ to $S_{350\text{-}400}$.

To describe changes in CDOM spectral properties along with change in CDOM concentration, the following equation was used:

$$S_{275-295} = \alpha + \beta/a_{CDOM}(325); \quad (2)$$

where α and β are the regression coefficients.

The variability of the relationship $a_{CDOM}(325)/DOC$ vs $S_{275-295}$, as possible tool for DOC estimation from spectroscopic measurements, was expressed as:

$$a_{CDOM}(325)/DOC = e^{(\gamma-\delta S_{275-295})} + e^{(\varepsilon-\zeta S_{275-295})}; \quad (3)$$

where γ, δ, $\varepsilon$and ζ are regression coefficients.

2.3.2 FDOM

The 3D fluorescence spectra were corrected for spectral bias, background signals and inner filter effects. Each EEM was normalized to the area of the ultra-pure water Raman peaks,

measured in the same day. EEMs were combined into three-dimensional data array, analyzed by PARAFAC (Stedmon and Bro, 2008) and validated by split-half analysis using "drEEM toolbox for MATLAB" after Murphy et al. (2013).

Only up to three components could be validated. For models with more than three components the results varied during split-half analysis (see Murphy et al., 2013), indicating the possibility of identifying the instrument noise as a signal (e.g. Stedmon and Markager, 2005). The fluorescence of each component is stated as fluorescence at excitation and emission maximums in Raman units (RU).

2.3.3 Mesocosm data treatment

Based on the nutrient component that was mainly varied, the experiments are referred to as Varied P and Varied N in the following.

High variability of CDOM components (Fig.S1) was observed on day 1 and day 2 of Varied P and day 1 of Varied N. This variability was likely associated to the filling and manipulation of the mesocosm bags and vanished afterwards. These days were excluded from further calculations, and day 3 and day 2 were defined as "start" or "beginning" of Varied P and Varied N, respectively. Day 8 was defined as the "end*"* of both experiments. To exclude initial variability, changes of the different DOM parameters over time were calculated as the difference between sampling day and start day:

$$\Delta Ci(k) = Ci(k) - Ci(start); \quad (4)$$

where C is a concentration, absorption or fluorescence intensity, i is a mesocosm id ($i = 1 - 16$) and k is the day of experiment.

For the presentation of the development over time, POM and DOM Δ-values were averaged for each nutrient treatment.

The 'cornerpoints' are not presented in the DOM development plots, since both DIN and DIP in them were modified. Therefore, including these treatments could bias the interpretation of effects induced by single inorganic nutrients. However, in plots and analyses where DIP or DIN influence was investigated all treatments were included to avoid a single nutrient effect overestimation.

For an estimation of the drivers of changes in DOM optical properties, the covariance of total accumulation of DOM compounds (Δ_8DOM) with the cumulative sum of POM (Σ_{POM}) parameters was tested by linear regression analysis.

Mean normalized deviations (mean dev. %), calculated as:

$$mean\ dev\ \% = \frac{100}{\overline{\Delta C} n} \sum_{start}^{end} \Delta Ci(k) - \overline{\Delta C(k)}; \quad (5)$$

where C- is a concentration, absorption or fluorescence intensity, k – is the day of experiment, n – is a total number of days ($n = end - start$) and i - is a mesocosm ID ($i = 1 - 16$); $\Delta Ci(k)$ is calculated by equation (4), $\overline{\Delta C(k)}$ – is the mean ΔC for all mesocosms at the day k, and $\overline{\Delta C}$ – is average ΔC for all mesocosms during the whole experiment. Mean dev. (%) were tested against nutrient supply (Varied P and Varied N) and DIN:DIP supply ratio in the mesocosms at day 2 in order to estimate the nutrient and stoichiometry effect on DOM accumulation in the mesocosms.

All statistical tests in this work were performed by the use of Sigma Plot 12.0 (Systat). The significance level was $p < 0.05$.

3. Results

3.1 Particulate organic matter development

After nutrient addition, a phytoplankton bloom development was observed in all mesocosms during both experiments. Maximum chl *a* concentrations in Varied P occurred at day 5 (Fig.1a), with higher concentrations in treatments with initial nutrients supplied at lower or equal to Redfield N:P ratio (12.00N/0.75P, 12.00N/1.25P, 12.00N/1.75P). However, no significant relationship of the cumulative sums of chl *a* ($\Sigma_{chl\ a}$) to DIP concentration was recognized (p>0.05, n=15). In Varied N, chl *a* concentrations reached its maximum at day 6 (Fig.1b) and $\Sigma_{chl\ a}$ were significantly affected by the initial DIN concentrations (Wilcoxon rank test: p<0.001, n=16), indicating that DIN was regulating phytoplankton biomass buildup.

Bacterial abundance increased until day 6 (paired t-test: p>0.001, n=31) in all mesocosms and then stayed relatively constant towards the end of both experiments (paired t-test: p>0.05, n=31; Fig.1c, d). In Varied P, cumulative sums of bacterial abundance (Σ_{bac}) were not related to the initial DIP supply (p>0.05, n=15). Highest bacterial abundance was observed at day 6, yielding $2.0\pm0.7 \times 10^6$ mL^{-1} averaged for all treatments (Fig.1c). In contrast, in Varied N, Σ_{bac} was significantly positively correlated to DIN amendments (p<0.01, n=16). The highest bacterial abundance of $2.6\pm0.2 \times 10^6$ mL^{-1} was observed at day 6 in the treatment with the highest initial DIN concentration (20.00N/0.75P).

3.2 Dissolved organic matter

3.2.1 Dissolved organic matter concentration

The initial DOC concentration (day 3), did not differ significantly between treatments in Varied P (one way ANOVA: p>0.05, n=15) and was 99±5 µmol L^{-1} on average. In contrast, in Varied N initial DOC concentrations (day 2) varied significantly among treatments (Holm-Sidak test: p<0.001, n=16) with 87±2 µmol L^{-1} in the treatment with second lowest initial DIN concentrations (4.00N/0.75P), 91±1 µmol L^{-1} on average for the Redfield DIN:DIP treatment (12.00N/0.75P) and for the treatment with the lowest initial DIN concentrations (2.00N/0.75P), and 95±3 µmol L^{-1} in the treatment with the highest initial DIN concentrations (20.00N/0.75P). The calculation of DOC accumulation (ΔDOC) thus allowed a better comparison of bulk DOC dynamics between treatments than absolute concentrations and will be given in the following.

During both experiments, DOC accumulated significantly over time (paired t-test of start and end values: p<0.001, n=15 and 16, respectively) with generally higher accumulation observed

in Varied N than in Varied P (Mann-Whitney rank sum test: p<0.001, n=120). On day 8, accumulation of DOC (Δ_8DOC) was highest (33±23 µmol L^{-1}) in the highest DIP treatment (12.00N/1.75P) in Varied P (Fig.2a), as well as in the highest DIN treatment (20.00N/0.75P) in Varied N (67±3 µmol L^{-1}) (Fig.2b).

Initial average CDOM absorption at 325 nm ($a_{CDOM}(325)$) was 0.17±0.03 m^{-1} and 0.15±0.01 m^{-1} for mesocosms of Varied P and Varied N, respectively (Fig.S1c, d). For both experiments, the starting CDOM absorption values were not significantly different between treatments (one way ANOVA: p>0.05, n=15 and p>0.05, n=16). However, they differed between the two experiments (one way ANOVA: p<0.05, n=31). CDOM accumulation ($\Delta a_{CDOM}(325)$) will be given in the following, as it allows a better comparison of CDOM dynamics between experiments than absolute absorption coefficients.

CDOM accumulated over time during both experiments (paired t-test of start and end values: p<0.001, n=15 and p<0.001, n=16, respectively). CDOM accumulation on day 8 ($\Delta_8 a_{CDOM}(325)$) was highest in the medium to high DIP treatment (12.00N/0.75P, 12.00N/1.25P, 12.00N/1.75P) in Varied P (0.35±0.03 m^{-1}) (Fig.2c) and in the highest DIN treatment (20.00N/0.75P) in Varied N (0.48±0.13 m^{-1}) (Fig.2d).

Spectral slopes, calculated within the 275-295 nm spectral range, ($S_{275\text{-}295}$) differed between treatments in the beginning of Varied N (one way ANOVA: p<0.05, n=16), whereas treatments in the beginning of Varied P were not significantly different (one way ANOVA: p>0.05, n=15). In order to avoid the influence of initial differences of spectral slopes on data analyses, daily changes in spectral slopes ($\Delta S_{275\text{-}295}$) were calculated. More negative $\Delta S_{275\text{-}295}$ indicate that the spectral slope is decreasing. As the spectral slope decreased, CDOM absorption at longer wavelengths became higher, indicating accumulation of HMW CDOM.

$S_{275\text{-}295}$ decreased over time in both experiments (paired t-test of start and end values: p<0.01, n=15 and p<0.01, n=16, for Varied P and Varied N respectively). The most negative $\Delta S_{275\text{-}295}$ values (-0.016±0.004 nm^{-1} and -0.014±0.002 nm^{-1}) were observed in the treatments with medium and high initial DIP concentrations (12.00N/0.75P, 12.00N/1.25P, 12.00N/1.75P) at the end (day 8) of Varied P (Fig.2e) and in the treatment with the highest initial DIN concentrations (20.00N/0.75P) in at the end (day 8) of Varied N (Fig.2f), respectively. In general, $\Delta S_{275\text{-}295}$ decreased faster in treatments with medium and high initial DIP concentrations (12.00N/0.75P, 12.00N/1.25P, 12.00N/1.75P) in Varied P and in treatment with the highest initial DIN concentrations (20.00N/0.75P) in Varied N (Table 2).

In the relationship between $S_{275\text{-}295}$ and $a_{CDOM}(325)$ no apparent differences between treatments were found. The relationship could be explained by equation (2) with $\alpha = 0.022$ and $\delta = 0.0035$ (Fig.3).

The S_R had much larger uncertainties within treatments than spectral slopes themselves. The initial S_R (day 3 and day 2) was not statistically different among treatments in each experiment (one way ANOVA: $p>0.05$, $n=15$ and 16, respectively) and between experiments (one way ANOVA: $p>0.05$, $n=31$).

S_R increased only slightly over time in almost all mesocosms of Varied P (paired t-test of start and end values: $p<0.05$, n=15; Fig.2g). In Varied N, S_R increased significantly on day 5 (paired t-test of start and day 5 values: $p<0.001$, n=16) and decreased again slightly on day 7 (paired t-test of day 5 and day 7 values: $p<0.05$, n=16) in almost all mesocosms (Fig.2h).

Three FDOM components with distinct spectral properties were identified during PARAFAC analysis of our dataset. The first FDOM component (Comp.1) was excited at 235 nm and emitted at 440-460 nm, the second (Comp.2) and the third (Comp.3) FDOM components were excited at 275 and 265 nm and emitted at 340 and 294 nm respectively. Both also had secondary excitation peaks at wavelength less than 230 nm (Table 3, Fig.4).

The initial fluorescence of Comp.1 was 0.019±0.001 Raman Units (RU) in Varied P and 0.0108±0.0009 RU in Varied N. Initially, Comp.1 fluorescence was not significantly different between treatments in both, Varied P and Varied N (one way ANOVA*:* $p>0.05$, $n=15$ and $p>0.05$, $n=16$, respectively) in contrast to initial differences between two experiments (one way ANOVA: $p<0.01$, $n=31$).

Subtracting the initial fluorescence of Comp.1 (ΔComp.1) allowed tracing the accumulation of freshly-produced Comp.1 during the experiments (Fig.2i, j).

ΔComp.1 indicated an accumulation of Comp.1 over time in both experiments (paired t-test of start and end values: $p<0.001$, $n=15$ and $p<0.001$, $n=16$). In Varied P, differences in ΔComp.1 fluorescence between treatments at the end of the experiment were not significant (t-test: $p>0.05$, $n=6$) and revealed 0.014±0.004 RU on the average for all mesocosms (Fig.2i). In Varied N, the highest ΔComp.1 fluorescence intensities of 0.025±0.004 RU were found in the treatment with the highest DIN supply (20.00N/0.75P) (Fig.2j). Here, clear differences were observed between treatments at the end of the experiment (one way ANOVA: $p<0.01$, $n=8$).

The fluorescence intensities of Comp.2 were almost identical at the start of Varied P and Varied N, yielding 0.029±0.005 RU and 0.029±0.007 RU, respectively. No significant

differences were observed between treatments (one way ANOVA: $p>0.05$, $n=15$ and $p>0.05$, $n=16$, for Varied P and Varied N respectively) and experiments (one way ANOVA: $p>0.05$, $n=31$).

Comp.2 fluorescence increased in all mesocosms over time (paired t-test of start and end values: $p<0.001$, $n=15$ and $p<0.001$, $n=16$) (Fig.2k, l). At the end (day 8) of Varied P, the maximum ΔComp.2 fluorescence was 0.063±0.007 RU in the treatment with highest DIP addition (12.00N/1.75P) (Fig.2k). At day 8, it was significantly higher than that in the treatment with the lowest initial DIP concentration (12.00N/0.25P) (t-test: $p<0.05$, $n=6$). Differences between treatments with the highest (20.00N/0.75P) and the lowest (2.00N/0.75P) initial DIN concentrations at the end (day 8) of Varied N were not significant (t-test: $p>0.05$, $n=6$) and the maximum ΔComp.2 fluorescence comprised 0.04±0.03 RU on average for all mesocosms (Fig.2l).

The Comp.3 fluorescence intensity was highly variable during both experiments (Fig.2m, n). Its starting values were not statistically different between Varied P and Varied N (two way ANOVA: $p>0.05$, $n=31$) and comprised 0.03±0.02 RU in both.

In Varied P, Comp.3 fluorescence intensity increased from start until day 5 (paired t-test of start and day 5 values: $p<0.05$, $n=15$) and decreased after day 6 until end of experiment (paired t-test of day 5 and end values: $p<0.05$, $n=15$) (Fig.2m). In Varied N, Comp.3 accumulated significantly only after day 6 (paired t-test of day 6 and end values: $p<0.05$, $n=16$) (Fig.2n).

3.2.2 Assessing the origin of optically active dissolved organic matter

To investigate a potential influence of phytoplankton or bacteria abundances on DOC concentrations and CDOM and FDOM accumulation, cumulative sums of chl *a* ($\Sigma_{chl\ a}$) and bacterial abundance (Σ_{bac}) of each mesocosm (Section S2) were tested against total accumulation of DOM components at day 8 (Δ_8DOM) using linear regression analysis.

Values of Δ_8DOC correlated significantly with $\Sigma_{chl\ a}$ in Varied P ($p<0.05$, $n=15$) and in Varied N ($p<0.001$, $n=16$), but not with Σ_{bac} ($p>0.05$, $n=15$ and $p>0.05$, $n=16$, respectively).

CDOM accumulation ($\Delta_8 a_{CDOM}(325)$) correlated significantly to $\Sigma_{chl\ a}$ in Varied P ($p<0.05$, $n=15$) and Varied N ($p<0.001$, $n=16$), indicating that phytoplankton biomass was regulating CDOM dynamics in both experiments. While no covariance of $\Delta_8 a_{CDOM}(325)$ with Σ_{bac} was observed during Varied P ($p>0.05$, $n=15$), a significant correlation of $\Delta_8 a_{CDOM}(325)$ with Σ_{bac}

(p<0.05, n=16) occurred in Varied N, indicating that bacteria may be partially responsible for CDOM dynamics under DIN stimulation.

ΔComp.1 behaved similar to $\Delta_8 a_{CDOM}(325)$ during both experiments. However, Δ_8Comp.1 was neither correlated to Σ_{bac} (p>0.05, n=15), nor to $\Sigma_{chl\ a}$ concentration (p>0.05, n=15) in Varied P. In contrast Δ_8Comp.1 was significantly correlated to both, $\Sigma_{chl\ a}$ (p<0.001, n=16) and Σ_{bac} (p<0.05, n=16) in Varied N.

Similar to Δ_8Comp.1, in Varied P, Δ_8Comp.2 did not reveal a significant relationship to $\Sigma_{chl\ a}$ (p>0.05, n=15) concentration or to Σ_{bac} (p>0.05, n=15). In Varied N, Δ_8Comp.2 also did not correlate to $\Sigma_{chl\ a}$ concentration (p>0.05, n=16), but it covariate significantly to Σ_{bac} (p<0.01, n=16), supporting a potential influence of bacterial abundance on fluorescence intensities of Comp.2.

In contrast to Δ_8Comp.1 and Δ_8Comp.2, Δ_8Comp.3 did not covariate, neither with Σ_{bac} (p>0.05, n=15 and p>0.05, n=16), nor with $\Sigma_{chl\ a}$ concentration (p>0.05, n=15 and p>0.05, n=16) in both experiments.

3.2.3 Effect of inorganic nutrients on optically active DOM

To assess the nutrient influence on DOM accumulation, mean normalized deviations (mean dev. %) of ΔDOC, ΔCDOM ($\Delta a_{CDOM}(325)$) and ΔFDOM were calculated for each mesocosm (including "corner" points) and tested against initial DIP supply in Varied P, and against initial DIN supply in Varied N using linear regression analysis (Fig.5), and also against DIN:DIP ratio combining both experiments.

DOC accumulation was related to the initial inorganic nutrient supply in both experiments. Higher ΔDOC (mean dev. %) corresponded to higher DIP supply (p<0.05, n=15) in Varied P (Fig. 5a) and to higher DIN supply (p<0.05, n=16) in Varied N (Fig. 5b). However, no overall effect of DIN:DIP ratios was revealed when data from both experiments were combined (p>0.05, n=31). Therefore, accumulation of DOC, in general, was dependent rather on total initial amount of macronutrients, than on the relative concentration of DIN to DIP.

ΔCDOM (mean dev. %) correlated significantly to DIN supply (p<0.001, n=14) (Fig.4c), but not to DIP supply (p>0.05, n=15) (Fig.5d). Similar to ΔDOC (mean dev. %), no effect of initial DIN:DIP ratios on ΔCDOM (mean dev. %) was determined (p>0.05, n=31).

ΔComp.1 (mean dev. %) did not exhibit a significant relationship to the initial DIP supply (p>0.05, n=15) (Fig.5e), but correlated significantly to the initial DIN concentrations (p<0.001, n=12) (Fig.5f).

Oppositely, ΔComp.2 (mean dev. %) increased with initial DIP supply (p<0.05, n=14) (Fig.5g), but not with initial DIN supply (p>0.05, n=12) (Fig.5h). Thus, Comp.2 accumulation was higher under the higher DIP concentrations.

In contrast to both previous FDOM components, ΔComp.3 (mean dev. %) did not reveal covariance neither to DIP (p>0.05, n=15) (Fig.5i), nor to DIN (p>0.05, n=12) initial supply (Fig.5n).

No overall effect of DIN:DIP ratios on ΔComp.1, ΔComp.2 and ΔComp.3 (mean dev. %) was determined when data from both experiments were combined (p>0.05, n=27, p>0.05, n=27 and p>0.05, n=27, respectively).

Hence, accumulation of Comp.1 was dependent on the initial DIN concentrations, accumulation of Comp.2 increased with increase of initial DIP concentrations and Comp.3 was unaffected by nutrient treatments.

3.2.4 Nutrients effects on the relationship between CDOM and DOC

To investigate the relationship between CDOM absorption and DOC concentrations during the course of the experiments, daily DOM accumulation (ΔDOC) was tested against daily accumulation of CDOM at 325 nm ($\Delta a_{CDOM}(325)$) by linear regression analysis for each mesocosm and for all data combined (Fig.6a, b). Direct overall relationships were observed between ΔDOC and $\Delta a_{CDOM}(325)$ in both, Varied P (p<0.001, n=75) and Varied N (p<0.001, n=95).

The estimated slopes of linear regressions, determined for each mesocosm for $\Delta a_{CDOM}(325)$ vs ΔDOC ($d\Delta a_{CDOM}(325)/d\Delta DOC$), were tested for correlation with the initial DIP (Fig.6c) and DIN (Fig.6d) concentration, in Varied P and Varied N, respectively. The $d\Delta a_{CDOM}(325)/d\Delta DOC$ significantly increased with an increase of initial DIN supply (p<0.01, n=16), indicating that the colored fraction of DOC was affected by nutrient availability, specifically by DIN supply.

Although the relationship between CDOM and DOC revealed a dependency on initial DIN supply, the values of $a_{CDOM}(325)$ to DOC ratio ($a_{CDOM}(325)$/DOC) did not reveal a significant nutrient effect, when plotted against $S_{275\text{-}295}$ (Fig.6e).

All data of $S_{275\text{-}295}$ and $a_{CDOM}(325)$/DOC of our study could be described by the equation (3), with coefficients γ, δ, ε and ζ equal to 5.67, 81.23, 3.18 and 23.03, respectively (Fig.6e).

4. Discussion

4.1 Nutrient effects on the production and cycling of optically active DOM

Our results indicate that chl *a* accumulation and bacterial growth were stimulated by DIN supply. Along with the response of POM production to inorganic nutrient amendments, changes in the optically active DOM fractions were observed.

Initial DOC concentrations, measured in both experiments (Fig.S1a, b), were in the range or slightly higher of those previously reported and modelled for the upper 30 m of the Tropical Atlantic Ocean watercolumn (Hansell et al., 2009).

In both experiments, DOC accumulated over time (Fig. 2a, b) and seemed to be produced mainly through phytoplankton release. The highest DOC accumulation was observed on the moment of rapid transition from nutrient replete to nutrient depleted conditions (see also Engel et al., 2015). That is in line with previous studies (Engel et al., 2002, Conan et al., 2007, Carlson and Hansell, 2015) showing DOM accumulation after the onset of nutrient limitation, while the chl *a* signal decreased.

The effect of initial nutrient concentrations on DOC accumulation (Fig. 5a, b), observed in our study, was shown previously. In a mesocosm study with ETNA waters, Franz et al. (2012) observed that higher DOC concentrations developed when the initial inorganic nitrogen supply was high. As well, DOC concentrations in their study were even higher when high DIN concentrations were combined with high DIP supply. In their mesocosm experiment in Raunefjord, Conan et al. (2007) and Stedmon and Markager (2005) observed that at silicate-replete conditions, DOC concentrations under high initial DIN supply did not vary significantly from those under high initial DIP concentrations. In our study, silicate was also not limiting phytoplankton growth and higher DOC concentrations occurred at higher DIP as well as at higher DIN concentrations, supporting earlier findings.

Bacterial turnover may have influenced the composition of DOM (as it is seen by changes in spectral slope ratios and FDOM components) while DOC concentrations seemed to be not related to bacterial abundances. This observation may be explained by rapid bacterial consumption of labile DOM accompanied by the bacterial release of altered humic-like DOM (Azam et al., 1983, Ogawa et al., 2001), which are therefore not influencing measured DOC concentrations (e.g. Kirchman, 1991).

At the beginning of the experiment, CDOM absorption coefficients were in the range of those previously reported for open waters of the Atlantic Ocean, while the final CDOM absorptions

were twice as high (Fig.S1c, d; Andrew et al., 2013, Nelson and Siegel, 2013). Similar to our experiments, CDOM absorption was previously shown to accumulate by factor of 2 during mesocosm studies, such as study by Pavlov et al. (2014), where nutrient levels for DIN were kept at 5 µmol L^{-1} and 0.32 µmol L^{-1} for DIP.

In our experiments, the accumulation of CDOM during the phytoplankton bloom (Fig. 2c, d) as well as significant covariance to phytoplankton pigment – chl *a* - concentration suggests that phytoplankton was the major source of CDOM. This is consistent with previous studies that show CDOM to be produced by extracellular release from phytoplankton (Romera-Castillo et al., 2010) or by phytoplankton degradation or lysis (Hu et al., 2006, Zhang et al., 2009, Organelli et al., 2014).

The decrease of CDOM spectral slopes over time (Fig. 2e, f) along with the increase in CDOM concentrations (Fig.3) indicated that absorption in the visible wavelength range increased relatively to the UV wavelength range. As the absorption at longer wavelength is corresponding to larger molecules, we may assume that HMW-CDOM accumulated during both experiments. HMW-DOM was previously shown to be more labile for bacterial consumption than low molecular weight DOM (at molecular weight cutoff of 1 kDa) (Benner and Amon, 2015), as bacterial activity was higher, when incubating with HMW-DOM (Amon and Benner, 1996). Furthermore HMW-DOM is typically accounting for 30 to 60 % of the total DOM released via phytoplankton (Biddanda and Benner, 1997, Engel et al., 2011). Therefore, we consider the spectral slope decrease over time as an indication of labile CDOM production via phytoplankton release.

In treatments with high initial DIN concentrations, bacterial abundance was significantly higher than in those with lower initial DIN concentrations. Furthermore, bacterial abundances in Varied N correlated significantly to CDOM concentrations. We therefore suggest that higher bacterial abundance may have been responsible for an additional production of CDOM in mesocosms, particularly in those with high initial DIN supply.

This suggestion is made also based on changes in optical properties during our study. As Helms et al (2008) and Zhang et al. (2009) showed before, the spectral slope ratio (S_R) decreases, when bacterial modification of CDOM takes place. A slight decrease of S_R towards the end of Varied N (Fig.2 h), most likely indicated that CDOM was reworked by bacteria. Our conclusion of additional CDOM production by bacteria in this experiment is also in agreement with previous studies, where DOM bacterial reworking was indicated as CDOM

source (Rochelle-Newall and Fisher, 2002, Kramer and Herndl, 2004, Nelson et al., 2004, Biers et al., 2007, Swan et al., 2009, Nelson and Siegel, 2013).

However, due to its large uncertainties within treatments, S_R was not sufficient to estimate the degree of bacterial CDOM production, most likely due to screening of the effect by simultaneous high HMW-DOM production via phytoplankton release. Therefore, CDOM production via phytoplankton release, which occurred proportionally to phytoplankton biomass, was likely more pronounced than CDOM production via bacterial reworking of labile DOM.

The CDOM to DOC ratio was also affected by variable initial DIN concentrations. A significant positive correlation of CDOM accumulation over time with DOC concentration was found in both experiments (Fig.6a, b), indicating that DOC and CDOM had been affected by the same processes. Estimated slopes of ΔCDOM against ΔDOC (Fig. 6d), in Varied N, were highest at highest initial DIN concentrations, indicating that relative proportion of CDOM in bulk DOM may be regulated by the presence of DIN.

Factors, influencing the ratio between CDOM absorption and DOC concentrations are little understood so far. It is known that CDOM absorption often co-varies with DOC concentration in river estuaries and coastal seas, which are influenced to a high degree by conservative mixing of riverine and marine waters (Nelson and Siegel, 2013, Rochelle-Newall et al., 2014). However, in the open ocean, the relation is losing its consistency (Nelson and Siegel, 2013). We suggest that under higher initial DIN concentrations bacterial abundance is higher and such is the bacterial reworking of DOM. Higher bacterial reworking, in its turn, causes an increase in the proportion of the colored fraction in DOM. Our results suggest that an increase of initial DIN concentrations by 10 µmol L^{-1} would cause an increase in CDOM accumulation ($\Delta a_{CDOM}(325)$) by 1.4 x 10^{-3} m^{-1} μmol^{-1} L (see Fig.6d) relative to accumulation of DOC (ΔDOC). The change, however, is small, compared to those, caused by other factors, as, for instance, mixing and photochemical oxidation (Stedmon and Nelson, 2015). Nonetheless, the effect may be important in regimes or at times, where or when changes of DIN concentrations are high.

When CDOM properties, such as spectral slopes $S_{275\text{-}295}$, were also taken into account, the variance of relationship between CDOM and DOC between treatments was not as apparent (Fig.6e). We found a good correspondence between $S_{275\text{-}295}$ and $a_{CDOM}(325)$/DOC ratio during our study, which could be explained by equation (3). Our data suggest, that the stable $S_{275\text{-}295}$ to $a_{CDOM}(325)$/DOC relationship could be used for DOC estimation in the open ocean, when

623 $S_{275\text{-}295}$ and $a_{CDOM}(325)$ are known, as, for instance, in field studies, where optical sensors are
624 used. For remote sensing, however, an application of this relationship would be rather
625 difficult, since ocean color remote sensing measurements are limited to an "optical window"
626 of visible to near-infrared wavelength range (Robinson, 2010).

627 Besides absorption, FDOM fractions were more sensitive to nutrient amendments. During our
628 study, three different fluorescent components could be identified (Fig.4).

629 The characteristics of the first component, Comp.1 (Table 3), were similar to those of the
630 humic-like peak 'A' described by Coble et al. (1996). The Comp.1 fluorescence was within
631 the reported range of A-like peak fluorescence intensities for the open ocean area (Jørgensen
632 et al., 2011) or slightly higher towards the end of experiments depending on mesocosm
633 treatment (Fig.S1i, j).

634 Marine humic substances were previously assigned to bacterially derived substances due to
635 significant covariance of their concentrations to apparent oxygen utilization in deep open
636 ocean waters (Swan et al., 2009, Kowalczuk et al., 2013, Nelson and Siegel, 2013). As well,
637 previous studies of Stedmon and Markager (2005), Kowalczuk et al. (2009) and Zhang et al.
638 (2009) showed that humic-like components, similar by spectral properties to Comp.1, were
639 produced via microbial DOM reworking (Table 3).

640 In our study, in Varied N, Comp.1 was strongly correlated to initial DIN concentrations, as
641 the final Comp.1 fluorescence intensity was almost three fold higher at the highest initial DIN
642 supply than that in the treatments with lowest DIN supply. Thus, since bacterial abundance
643 was DIN dependent in this experiment and Comp.1 fluorescence intensities correlated
644 significantly to bacterial abundances, the bacteria were likely responsible for Comp.1
645 occurrence during our experiments. The proportional to DIN bacterial production of humic-
646 like Comp.1 in our study is in agreement with Kramer and Herndl (2004) and Biers et al.
647 (2007), where DIN and its organic derivatives were considered to be the primary drivers of
648 humic-like DOM accumulation via bacterial reworking.

649 In Varied P, however, Comp.1 was not related to bacterial abundance. No significant
650 differences between treatments were noticed for bacterial abundance and only little
651 differences occured for Comp.1 at similar initial DIN supply concentrations. Thus, under
652 equal initial DIN concentrations bacterial reworking of DOM could occur at similar degree,
653 causing the absence of covariance of Comp.1 with bacterial abundance.

The higher concentrations of Comp.1 at the end of our experiments compared to concentrations measured in open ocean (Jørgensen et al., 2011) may be explained by slightly higher substrate availability in the mesocosms than that in the North Atlantic.

The fluorescence properties of the second FDOM component, Comp.2 (Table 3), were similar to that of the previously defined amino acid-like fluorescence (Mopper and Schulz, 1993, Coble et al., 1996, Stedmon and Markager, 2005): tryptophan-like peak 'T' (Coble et al., 1996). The fluorescence intensities of this component were in the range of that previously reported for open ocean area (Jørgensen et al., 2011) for the whole experimental period (Fig.S1k, l).

Similar by spectral properties to Comp.2, amino acid-like compounds were previously hypothesized to represent the fluorescence of the bound-to-protein matrix amino acids tryptophan and tyrosine (Stedmon and Markager, 2005) and were assumed to be produced by phytoplankton (Mopper and Schulz, 1993, Coble et al., 1996). We, therefore, consider Comp.2 as an indicator of phytoplankton-produced proteinaceous DOM and as possible precursor for humic-like FDOM.

In Varied P, Comp.2 accumulated proportionally to initial DIP concentrations and its concentration was not corresponding to chl *a* concentration. This might indicate that proteinaceous DOM release by phytoplankton is controlled by nutrient availability, rather than by phytoplankton biomass itself, i.e. proteinaceous DOM is produced as a part of an "overflow mechanism" (Wood and Van Valen, 1990) of extracellular release.

In Varied N, again no covariance of Comp.2 to chl *a* was determined. However, a covariance of Comp.2 with initial DIN concentrations did not occur as well. As bacteria were more abundant in treatments with higher initial DIN supply and also Comp.2 intensities revealed significant correspondence to bacteria, we suggest that bacterial reworking may have regulated Comp.2 fluorescence intensities, particularly under high initial DIN concentrations.

Previously, Stedmon and Markager (2005) showed an accumulation of a FDOM component, with spectral properties similar to Comp.2, during their mesocosm study treatments of high DIN and high DIP concentrations. This component was also shown to be consumed during dark and light incubations, when bacteria were added. Kirchman et al. (1991) showed that DOM uptake can be accompanied by a decrease in DIN concentrations, indicating the importance of DIN presence during bacterial reworking of labile DOM. Therefore, Comp.2 production might be dependent on initial DIP and DIN availability, similarly to the increase of DOC concentrations. As well as at high initial DIN concentrations, Comp.2 may serve a

687 substrate for developing bacteria, i.e. it can be consumed by bacteria that, in their turn, release
688 humic-like Comp.1.

689 The spectral properties of the third fluorescent component (Comp.3) were similar to that of
690 amino acid-like fluorescence (Table 3) (Mopper and Schulz, 1993, Coble et al., 1996,
691 Stedmon and Markager, 2005): tyrosine-like peak 'B' (Coble et al., 1996) and were in the
692 range of those previously reported for open ocean area (Jørgensen et al., 2011; Fig.S1m, n).

693 The development patterns as well as no clear response towards nutrient amendments of
694 Comp.3 made it very difficult to interpret.

695 In Varied P, Comp.3 fluorescence intensities were highest at the day of chl *a* maximum (Fig.
696 2m). Thus, Comp.3 could be released by phytoplankton at the growth phase, while after the
697 chl *a* maximum, rapid bacterial reworking of DOM or abiotic aggregation to Comp.2 could
698 remove Comp.3 from the mesocosms.

699 In Varied N, Comp.3 fluorescence intensities were generally low, but increased at the end of
700 experiment (Fig. 2n). Therefore, the process of bacterial Comp.2 reworking could lead to
701 Comp.3 release as byproduct at the final stage of Varied N. On the other hand, Comp.3
702 accumulation towards the end of this experiment could be a result of extracellular release of
703 higher amounts of amino acid-like substances, which accumulated under high DIN
704 concentrations within phytoplankton tissues during its growth.

705 A fluorescent substance, similar by spectral properties to Comp.3, was previously
706 hypothesized to represent the tryptophan and tyrosine in peptides by Stedmon and Markager
707 (2005), as it had been previously found accumulating during the denaturation of proteins
708 (Determann et al., 1998). In their study, Stedmon and Markager (2005) found no effect of
709 microbial reworking on the abundance of this fluorescence substance in the dark and light
710 incubations with bacteria. However, as this substance was removed during thier mesocosm
711 experiment, they hypothesized spontaneous abiotic aggregation or photochemically induced
712 flocculation as possible removal mechanisms.

713 We, therefore, conclude that Comp.3 potentially acted as an intermediate product during the
714 formation or degradation of proteinaceous Comp.2 in our study. Still, the interpretation of the
715 Comp.3 development remains speculative.

716 It was hypothesized previously that phosphorus limitation leads to accumulation of DOM
717 more resistant to microbial degradation (Kragh and Sondergaard, 2009), e.g. due to
718 phytoplankton extracellular release of this 'poor quality' DOM or limitation of bacterial DOM

consumption (Carlson and Hansell, 2015). Based on changes in optical DOM properties (S_R, Comp.1, Comp.2) in our study, we suggest that labile DOM in the ETNA accumulates proportionally to either DIN or DIP concentrations. However, the 'poor quality' DOM accumulates more under high DIN concentrations (i.e. phosphorus limitation), due to bacterial DOM reworking. And even though bacterial activity per cell might have been limited by phosphorus availability, higher bacterial abundance in treatments with higher initial DIN supply would lead to more pronounced net accumulation of more resistant to microbial degradation DOM.

Overall, the variances of CDOM and FDOM concentrations in the treatment with DIN:DIP of 16 (12.00N/0.75P) for each experiment were higher than the variance in this treatment between experiments. Therefore, the effects of nutrients on CDOM and FDOM concentrations were considered much stronger, than possible effects, caused by differences in initial sensitivity to nutrient additions. However, due to the divergence in development pattern for some of optically active parameters (S_R, Comp.3), we cannot exclude the difference in pelagic communities during Varied P and Varied N from the aspects that can cause an additional CDOM and FDOM variability during our study.

Another important aspect that could cause an additional CDOM and FDOM variability, and, therefore, bias the interpretation of obtained results during the mesocosm experiments, is the length of the sample storage. In our study, CDOM and FDOM samples were filtered through 0.45 µm pore-size filters and stored in the dark and cold (+4°C) for approximately 6 month pending analyses due to logistical reasons. This time-period is long and CDOM and FDOM concentrations could be affected by remained bacteria during storage. The long-term storage of open ocean CDOM samples has been tested previously by Swan et al. (2009). They demonstrated that the CDOM changes are unappreciable, when the storage of pre-filtered CDOM samples at 4°C does not exceed one year. Furthermore, during our study, FDOM samples from all the mesocosms were measured for day 4 of each experiment (31 samples in total) in approximately 3 month after main set of measurements has been accomplished. No drastic or appreciable changes in FDOM components concentrations have been noticed as they developed, e.g. neither between replicates, nor between treatments. Therefore, despite, the pore-sizes of our filters were larger, than those, used by Swan et al. (2009), we believe, that due to generally low CDOM and FDOM concentrations the error that could occur, would not majorly influence the CDOM and FDOM development patterns during our observations.

5. Conclusions

Our study shows that during phytoplankton blooms DOM is largely derived from phytoplankton, while its optical properties undergo considerable changes due to bacterial reworking. Thus, optically active proteinaceous substances are freshly produced by phytoplankton release. They are, however, consumed and reworked by bacteria, leading to accumulation of less-bioavailable optically active humic substances.

Our experiments indicate that DIN is the major macronutrient regulating the accumulation of bacterially originated optically active humic substances, while the accumulation of labile proteinaceous substances via phytoplankton is rather regulated by DIN and DIP. An input of humic substances can increase the CDOM/DOC ratio and therewith affect predictions of DOC concentration based on CDOM absorption. Still, a relationship between CDOM spectral properties and CDOM and DOC concentrations can be derived, which is not influenced by nutrient differences.

6. Acknowledgements

This study was supported SFB754 project, "Climate-Biogeochemical Interactions in the Tropical Ocean" DFG. We thank all participants of our Cabo Verde 2012 research stay for joint work during water sampling and handling of mesocosms and also N. Vieira for help with initial water sampling. We also thank I. Monteiro, M. Schütt and P. Silva for help with logistics.

We are very grateful to P. Kowalczuk for valuable comments during our PARAFAC analysis, J. Roa for DOC analyses, U. Pankin for nutrient measurements, and S. Endres, L. Galgani, R. Flerus and C. Löscher for helpful discussions during the manuscript writing. We are very thankful also to P. Kowalczuk and an anonymous referee for reviewing and commenting the manuscript, as well as to M. Mostofa for his short comment of the manuscript.

All data will be available at www.pangaea.de upon publication of the manuscript.

7. References

Amon, R.M.W. and Benner, R. Bacterial utilization of different size classes of dissolved organic matter, Limnol.Oceanogr. 41, 41-51, 1996.

Andrew, A.A., Del Vecchio, R., Subramaniam, A., Blough, N.V.: Chromophoric dissolved organic matter (CDOM) in the Equatorial Atlantic Ocean: Optical properties and their relation to CDOM structure and sourse, Mar. Chem. 148, 33-43, 2013.

Azam, F., Fenchel, T., Field, J.G., Gray, J.S., Meyer-Reil, L.A., and Thingstad, F.: The ecological role of water-column microbes in the sea, Mar. Ecol.Prog.Ser. 10, 257-263, 1983.

Benner, R. and Amon, RMW.: The size-reaktivity continuum of major bioelements in the ocean, Annu.Rev.Mar.Sci. 7, 2.1-2.21, 2015.

Biddanda, B. and Benner, R.: Carbon, nitrogen and carbohydrate fluxes during the production of particulate and dissolved organic matter by marine phytoplankton, Limnol.Oceanogr. 42, 506-518, 1997.

Biers, E.J., Zepp, R.G., Moran, M.A.: The role of nitrogen in chromophoric and fluorescent dissolved organic matter formation, Mar. Chem. 103, 46-60, 2007

Brandt, P., Bange, H.W., Banyte, D., Dengler, M., Didwischus, S.-H., Fischer, T., Greatbatch, R. J., Hahn, J., Kanzow, T., Karstensen, J., Körtzinger, A., Krahmann, G., Schmidtko, S., Stramma, L., Tanhua, T., and Visbeck M.: On the role of circulation and mixing in the ventilation of oxygen minimum zones with a focus on the eastern tropical North Atlantic, Biogeosc. 12, 489-512, 2015.

Bricaud, A., Morel, A., and Prieur L.: Absorption by dissolved organic matter of the sea (yellow substance) in the UV and visible domain, Limnol. Oceanogr. 26(1), 43-53, 1981.

Carlson, C.A. and Hansell, D.A.: DOM sourses, sinks, reactivity and budgets, In Biogeochemistry of marine dissolved organic matter 2nd ed. By Hansell, D.A. and Carlson, C.A., Elsevier, 2015

Coble, P.G.: Characterisation of marine and terrestrial DOM in seawater using excitation-emission matrix spectroscopy, Mar. Chem. 51, 325-346, 1996.

Coble, P.G: Marine optical biogeochemistry: The chemistry of ocean color, Chem.Reviews 107(2), 402–418, doi:10.1021/cr050350+, 2007.

807 Conan, P., Søndergaard, M., Kragh, T., Thingstad, F., Pujo-Pay, M., Williams, P.J. le B.,
808 Markager, S., Cauwet, G., Borch, N.H., Evans, D., and Riemann, B.: Partitioning of
809 organic production in marine plankton communities: The effects of inorganic nutrient
810 ratios and community composition on new dissolved organic matter, Limnol.Oceanogr.
811 52(2), 753-765, 2007.

812 De Haan, H. and De Boer, T.: Applicability of light absorbance and fluorescence as measures
813 of concentration and molecular size of dissolved organic carbon in humic Laken
814 Tjeukemeer Water Res. 21, 731-734, 1987.

815 Del Castillo C.E.: Remote sensing of organic matter in coastal waters, In "Remote sensing of
816 coastal aquatic Environments: Technologies, techniques and applications" by Miller, R.L.,
817 Del Castillo, C.E., and McKnee, B.A., Springer, 2007.

818 Del Vecchio, R. and Blough, N.V.: On the origin of the optical properties of humic
819 substances, Env. Sc.Technol. 38(14), 3885-3891, 2004.

820 Determann, S., Lobbes, J.M., Reuter, R., and Rullköter, J.: Ultraviolet fluorescence excitation
821 and emission spectroscopy of marine algae and bacteria, Mar.Chem. 62, 137-156, 1998

822 Engel A., Borchard, C., Loginova, A., Meyer, J., Hauss, H., and Kiko, R.: Effects of varied
823 nitrate and phosphate supply on polysaccharidic and proteinaceous gel particle production
824 during tropical phytoplankton bloom experiments, Biogeosciences 12, 5647-5665, 2015.

825 Engel, A., Goldthwait, S., Passow, U., and Alldredge A.: Temporal decoupling of carbon and
826 nitrogen dynamics in a mesocosm diatom bloom, Limnol.Oceanogr. 47(3), 753-761, 2002.

827 Engel, A., Händel, N., Wohlers, J., Lunau, M., Grossart, H.-P-, Sommer, U., and Riebesell,
828 U.: Effects of sea surface warming on the production and consumption of dissolved
829 organic matter during phytoplankton blooms: results from a mesocosm study, Journ.Pl.Res.
830 33(3), 357-372, 2011.

831 Fanning, K.A.: Nutrient provinces in the sea: Concentration ratios, and ideal covariation,
832 J.Geophys.Res. 97, 5693-5712, 1992.

833 Fichot, C.G. and Benner, R.: A novel method to estimate DOC concentrations from CDOM
834 absorption coefficients in coastal waters, Geophys.Res.Letters 38, L03610,
835 doi:10.1029/2010GL046152, 2011.

836 Fichot, C.G. and Benner, R.: The spectral slope coefficient of chromophoric dissolved organic
837 matter ($S_{275-295}$) as a tracer of terrigenous dissolved organic carbon in river-influenced

838 ocean margins, Limnol. Oceanogr. 57(5), 1453-1466, doi:10.4319/lo.2012.57.5.1453,
839 2012.

840 Franz, J.M.S., Hauss, H., Sommer, U., Dittmar, T., and Riebesell, U.: Production, partitioning
841 and stoichiometry of organic matter under variable nutrient supply during mesocosm
842 experiments in the tropical Pacific and Atlantic Ocean, Biogeosciences 9, 4629-4643,
843 doi:10.5194/bg-9-4629-2012, 2012.

844 Granskog, M.A., Macdonald, R.W., Mundy, C.J., and Barber, D.G.: Distribution,
845 characteristics and potential impacts of chromophoric dissolved organic matter (CDOM) in
846 Hudson Strait and Hudson Bay, Canada, Continental Shelf Res. 27, 2032-2050, 2007.

847 Gruber, N. and Sarmento, J.L.: Global patterns of marine nitrogen fixation and denitrification,
848 Gl.Biogeochem.Cycles 11(2), 235-266, 1997.

849 Guéguen, C. and Kowalczuk, P.: Colored dissolved organic matter in frontal zones, In I.
850 Belkin: Chemical Oceanography of Frontal Zones, Springer Verlag,
851 doi:10.1007/698_2013_244, 2013

852 Hansell, D.A., Carlson, C.A., Repeta, D.J., and Shitzer, R.: Dissolved organic matter in the
853 ocean: a controversy stimulated new insights, Oceanography 22, 202-211, 2009.

854 Hauss, H., Franz, J.M.S., Hansen, T., Struck, U., and Sommer, U.: Relative inputs of
855 upwelled and atmospheric nitrogen to the eastern tropical North Atlantic food web: Spatial
856 distribution of $\delta^{15}N$ in meso zooplankton and relation to dissolved nutrient dynamics Deep-
857 Sea Res. I 75, 135–145, doi: 10.1016/j.dsr.2013.01.010, 2013.

858 Helms, J.R., Stubbins, A., Ritchie, J.D., and Minor, E.C.: Absorption spectral slopes and
859 slope ratios as indicators of molecular weight, source, and photobleaching of chromophoric
860 dissolved organic matter, Limnol.Oceanogr. 53(3), 955-969, 2008.

861 Hu, C., Lee, Z., Muller-Karger, F.E., Carder, K.L., and Walsh, J.J.: Ocean color reveals phase
862 shift between marine plants and yellow substance, IEEE Geosci. Remote Sensing Letters
863 3(2), 262–266, 2006.

864 Ishii, S.K.L. and Boyer, T.H.: Behavior of Reoccurring PARAFAC Components in
865 Fluorescent Dissolved Organic Matter in Natural and Engineered Systems: A Critical
866 Review, Environ. Sci. Technol. 46, 2006-2017, doi:10.1021/es2043504, 2012.

867 Jayakumar, A., O'Mullan, G.D., Naqvi, S.W.A., and Ward, B.B.: Denitrifying Bacterial
868 Community Composition Changes Associated with Stages of Denitrification in Oxygen
869 Minimum Zones, Microb. Ecol. 58, 350–362, doi:10.1007/s00248-009-9487-y, 2009.

870 Jetten, M.S., Niftrik, L., Strous, M., Kartal, B., Keltjens, J.T., and Op den Camp, H.J.:
871 Biochemistry and molecular biology of anammox bacteria, Crit. Rev. Biochem. Mol. Biol.
872 44(2-3), 65-84., doi:10.1080/10409230902722783, 2009.

873 Jiao, N., Herndl, G.J., Hansell, D.A., Benner, R., Kattner, G., Wilhelm, S.W., Kirchman,
874 D.L., Weinbauer, M.G., Luo, T., Chen, F., and Azam, F.: Microbial production of
875 recalcitrant dissolved organic matter: long-term carbon storage in the global ocean, Nature
876 Reviews Microbiology 8, 593-599, doi:10.1038/nrmicro2386, 2010.

877 Jørgensen, L., Stedmon, C.A., Kragh, T., Markager, S., Middelboe, M., and Søndergaard, M.:
878 Global trends in the fluorescence characteristics and distribution of marine dissolved
879 organic matter, Mar. Chem. 126, 139-148, doi:10.1016/j,marchem.2011.05.002, 2011.

880 Karstensen, J., Stramma, L., and Visbeck, M.: Oxygen minimum zones in the eastern tropical
881 Atlantic and Pacific oceans, Progr.Oceanogr. 77, 331–350,
882 doi:10.1016/j.pocean.2007.05.009, 2008.

883 Karstensen, J., Fiedler, B., Schütte, F., Brandt, P., Körtzinger, A., Fischer, G., Zantopp, R.,
884 Hahn, J., Visbeck, M., and Wallace, D.: Open ocean dead-zone in the tropical North
885 Atlantic Ocean, Biogeosciences Discuss., 11, 17391-17411, doi:10.5194/bgd-11-17391-
886 2014, 2014

887 Kartal, B., Kuypers, M.M., Lavik, G., Schalk, J., Op den Camp, H.J., Jetten, M.S., and Strous,
888 M.: Anammox bacteria disguised as denitrifiers: nitrate reduction to dinitrogen gas via
889 nitrite and ammonium Environ, Microbiol. 9(3), 635–642, 2007.

890 Kieber, R.J., Li, A., and Seaton, P.J.: Production of nitrite from photodegradation of dissolved
891 organic matter in natural waters, Env.Sci.Technol. 33(7), 993-998, 1999.

892 Kieber, R.J., Zhou, X., and Mopper K.: Formation of carbonyl compounds from UV-induced
893 photodegradation of humic substances in natural waters: fate of riverine carbon in the sea,
894 Limnol.Oceanogr. 35, 1503-1515, 1990.

895 Kirchman, D.L., Suzuki, Y., Garside, C. and Duklow, H.W.: High turover rates of dissolved
896 organic carbon during a spring phytoplankton bloom, Letters to Nature 325, 612-614,
897 1991.

898 Kowalczuk, P., Durako, M.J., Young, H., Kahn, A.E., Cooper, W.J., and Gonsior, M.:
899 Characterisation of dissolved organic matter fluorescence in the South Atlantic Bight with
900 the use of PARAFAC model: interannual variability, Mar.Chem. 113(3-4), 182-196, 2009.

901 Kowalczuk, P., Tilstone, G.H., Zabłocka, M., Röttgers, R., Thomas, R.: Composition of
902 dissolved organic matter along and Atlantic Meridional Transect from fluorescence
903 spectroscopy and Parallel Factor Analysis, Mar. Chem. 157, 170-184, 2013.

904 Kragh, T. and Sondergaard, M.: Production and decomposition of new DOC by marine
905 plankton communities: carbohydrates, refractory components and nutrient limitation,
906 Biogeochemistry 96, 177-187, 2009.

907 Kramer, G.D. and Herndl, G.J.: Photo- and bioreactivity of chromophoric dissolved organic
908 matter produced by marine bacterioplankton, Aquat. Microb. Ecol. 36, 293-246, 2004.

909 Mathis, J. T., Pickart, R.S., Hansell, D.A., Kadko, D., and Bates N.R.: Eddy transport of
910 organic carbon and nutrients from the Chukchi Shelf: impact on the upper halocline of the
911 western Arctic Ocean, J. Geophys. Res. 112, C05011, doi:10.1029/2006JC003899,
912 2007.

913 McGillicuddy Jr., D. J., Anderson, L. A., Doney S. C., and Maltrud M. E.: Eddy-driven
914 sources and sinks of nutrients in the upper ocean: result from a 0.1° resolution model of the
915 north Atlantic, Glob. Geochem. Cycles 17, 1035, doi:10.1029/2002GB001987, 2003.

916 McGillicuddy Jr., D.J., Anderson, L.A., Bates, N.R., Bibby, T., Buesseler, K.O., Carlson,
917 C.A., Davis, C.S., Ewart, C., Falkowski, P.G., Goldthwait, S.A., Hansell, D.A., Jenkins,
918 W.J., Johnson, R., Kosnyrev, V.K., Ledwell, J.R., Li, Q.P., Siegel, D. A., and Steinberg,
919 D.K.: Eddy/wind interactions stimulate extraordinary mid-ocean plankton blooms, Science
920 316, 1021–26, doi: 10.1126/science.1136256, 2007.

921 Mopper, K. and Schultz, C.A.: Fluorescence as possible tool for studying the nature of water
922 column distribution of DOC components, Mar.Chem. 41, 229-238, 1993.

923 Mopper, K., Stubbins, A., Ritchie, J.D., Bialk, H.M., and Hatcher, P.G.: Advanced
924 instrumental approaches for characterization of marine dissolved organic matter:
925 Extraction techniques, mass spectrometry, and nuclear magnetic resonance spectroscopy,
926 Chem. Reviews 107, 419 – 442, doi: 10.1021/cr050359b, 2007.

927 Moran, M.A. and Zepp, R.G.: Role of photoreactions in the formation of biologically labile
928 compounds from dissolved organic matter, Limnol.Oceanogr. 42, 1307-1316, 1997.

Murphy, K.R., Stedmon C.A., Graeber, D., and Bro, R.: Fluorescence spectroscopy and multy-way techniques. PARAFAC, Anal. Methods 5, 6557-6566, doi:10.1039/c3ay41160e, 2013.

Nelson, N.B. and Siegel, D.A.: The Global Distribution and Dynamics of Chromophoric Dissolved Organic Matter, Annu. Rev. Mar. Sci. 5, 447-476, doi: 10.1146/annurev-marine-120710-100751, 2013.

Nelson, N.B., Siegel, D.A., and Steinberg, D.K.: Production of dissolved organic matter by Sargasso Sea microbes, Mar. Chem., 89, 273-287, doi:10.1016/j.marchem.2004.02.017, 2004.

Nelson, N.B., Siegel, D.A., Carlson, C.A., Swan, C.M., Smethie, W.M., and Khatiwala, S.: Hydrography of chromophoric dissolved organic matter in the North Atlantic Deep-Sea Res.I 54, 710-731, doi:10.1016/j.dsr.2007.02.006, 2007.

Ogawa, H., Amagai, Y., Koike, I., Kaiser, K., and Benner, R.: Production of refractory dissolved organic matter by bacteria, Science 292, 917-920, 2001.

Organelli, E., Bricaud, A., Antoine, D., and Matsuoka, A.: Seasonal dynamics of light absorption by chromophoric dissolved organic matter (CDOM) in the NW Mediterranean Sea (BOUSSOLE site), Deep-Sea Res. I 91(2014)72–85, doi:10.1016/j.dsr.2014.05.003, 2014.

Parsons, T.R., Maita, Y., and Lalli, C.M.: A manual of chemical and biological methods for seawater analysis, Pergamon Press Oxford, UK, p.173, 1984.

Pavlov, A.K., Silyakova, A., Granskog, M.A., Bellerby, R.G.J., Engel, A., Schulz, K.G., and Brussaard, C.P.D.: Marine CDOM accumulation during a coastal Arctic mesocosm experiment: No response to elevated pCO_2 levels, Biogeosciences 119(6), 1216-1230, doi:10.1002/2013JG002587, 2014.

Redfield, A.C.: The biological control of chemical factors in the environment, Am.Sci. 46, 205-221, 1958.

Robinson, I. S.: Discovering the ocean from space: The unique applications of satellite oceanography, Springer, 2010

Rochelle-Newall, E.J. and Fisher, T.R.: Production of chromophoric dissolved organic matter fluorescence in marine and estuarine environments: An investigation into the role of phytoplankton, Mar.Chem. 77, 7-21, 2002.

960 Rochelle-Newall, E.J., Hulot, F.D., Janeau, J.L., and Merroune, A.: CDOM fluorescence as a
961 proxy of DOC concentration in natural waters: a comparison of four contrasting tropical
962 systems, Environ.Monit.Assess 186, 589-596, doi:10.1007/s10661-013-3401-2, 2014.

963 Romera-Castillo, C., Sarmento, H., Álvarez-Salgado, X.A., Gasol, J.M., and Marrase C.:
964 Production of chromophoric dissolved organic matter by marine phytoplankton,
965 Limnol.Oceanogr., 55(1), 446-454, 2010.

966 Stedmon, C.A. and Álvarez-Salgado, X.A.: Shedding Light on a Black Box: UV-Visible
967 Spectroscopic Characterization of Marine Dissolved Organic Matter, In Microbial Carbon
968 Pump by Jiao, N. and Azam, F., Senders, 2011.

969 Stedmon, C.A. and Bro R.: Characterizing dissolved organic matter fluorescence with parallel
970 factor analysis: a tutorial, Limnol. Oceanogr.: Methods 6, 572-579,
971 doi:10.4319/lom.2008.6.572, 2008.

972 Stedmon, C.A. and Markager S.: Tracing the production and degradation of autochtonous
973 fractions of dissolved organic matter by fluorescence analysis, Limnol.Oceanogr. 50(5),
974 1415-1426, 2005.

975 Stedmon, C.A. and Markager, S.: The optics of chromophoric dissolved organic matter
976 (CDOM) in the Greenland Sea: An algorithm for differentiation between marine and
977 terrestrially derived organic matter, Limnol. Oceanogr. 46(8), 2087-2093, 2001.

978 Stedmon, C.A. and Nelson, N.: The optical properties of DOM in the ocean, In
979 Biogeochemistry of marine dissolved organic matter 2nd ed. By Hansell, D.A. and Carlson,
980 C.A., Elsevier, 2015

981 Stedmon, C.A., Amon, R.M.W., Rinehart, A.J., and Walker, S.A.: The supply and
982 characteristics of colored dissolved organic matter (CDOM) in the Arctic Ocean: Pan
983 Arctic trends and differences, Mar. Chem. 124, 108-118, 2011.

984 Strous, M., Pelletier, E., Mangenot, S., Rattei, T., Lehner, A., Taylor, M.W., Horn, M.,
985 Daims, H., Bartol-Mavel, D., Wincker, P., Barbe, V., Fonknechten, N., Vallenet, D.,
986 Segurens, B., Schenowitz-Truong, C., Médigue, C., Collingro, A., Snel, B., Dutilh, B.E.,
987 Op den Camp, H.J.M., van der Drift, C., Cirpus, I., van de Pas-Schoonen, K.T., Harhangi,
988 H.R., Lan Niftrik, L., Schmid, M., Keltjens, J., van de Vossenberg, J., Kartal, B., Meier,
989 H., Frishman, D., Huynen, M.A., Mewes, H.-W., Weissenbach, J., Jetten, M.S.M.,
990 Wagner, M., and Le Paslier, D.: Deciphering the evolution and metabolism of an anammox

bacterium from a community genome, Nature 440, 790-794, doi:10.1038/nature04647, 2006.

Sugimura, Y. and Suzuki, Y.: A high-temperature catalytic oxidation method for the determination of non-volatile dissolved organic carbon in seawater by direct injection of a liquid sample, Mar. Chem. 24, 105–131, 1988.

Sulzberger, B. and Durisch-Kaiser, E.: Chemical characterization of dissolved organic matter (DOM): A prerequisite for understanding UV-induced changes of DOM absorption properties and bioavailability, Aquat.Sci. 71, 104-126, doi: 10.1007/s00027-008-8082-5, 2009.

Swan, C.M., Nelson, N.B., Siegel, D.A., and Fields, E.A.: A model for remote estimation of ultraviolet absorption by chromophoric dissolved organic matter based on global distribution of spectral slope, Remote Sensing of Environment 136, 277-285, doi:10.1016/j.rse.2013.05.009, 2013.

Swan, C.M., Siegel, D.A., Nelson, N.B., Carlson, C.A., and Nasir, E.: Biogeochemical and hydrographic controls on chromophoric dissolved organic matter distribution in the Pacific Ocean, Deep-Sea Res. I 56, 2172-2192, doi:10.1016/j.dsr.2009.09.002, 2009.

Wood, A. and Van Valen, L.,Paradox lost? On release of energy-rich compounds by phytoplankton, Mar. Microb. Food Webs 4, 103-116, 1990.

Yamashita, Y., Cory, R.M., Nishioka, J., Kuma, K., Tanoue, E., and Jaffé, R.: Fluorescence characteristics of dissolved organic matter in the deep waters of Okhotsk Sea and northweastern North Pacific Ocean, Deep-Sea Res. II 57, 1478-1485, doi:10.1016/j.dsr2.2010.02.016, 2010.

Yamashita, Y., Jaffe, R., Maie, N., and Tanoue, E.: Assessing the dynamics of dissolved organic matter (DOM) in coastal environments by excitation emission matrix fluorescence and parallel-factor analysis (EEM-PARAFAC), Limnol.Oceanogr. 53(5), 1900-1908, 2008.

Zepp, R.G., Shank, G.C., Stabenau, E., Patterson, K.W., Cyterski, M.J., Fisher, W.S., Bartels, E., and Anderson S.L.: Spatial and temporal variability of solar ultraviolet exposure of coral assemblages in the Florida Keys: Importance of Colored Dissolved Organic Matter, Limnol.Oceanogr. 53(5), 1909-1922, 2008

1021 Zhang, Y., van Dijk, M.A., Liu, M., Zhu, G., and Qin, B.: The Contribution of phytoplankton
1022 degradation to chromophoric dissolved organic matter (CDOM) in eutrophic shallow lakes:
1023 Field and experimental evidence, Water Research 43, 4685-4697,
1024 doi:10.1016/j.waters.2009.07.024, 2009.

1025

Table1. Varied P and Varied N: target concentrations and measured concentrations of DIN and DIN and treatment identifications according to target nutrients concentrations.

Mesocosm ID	Varied P					Varied N				
	target		Measured		Treatment	target		measured		Treatment
	DIN	DIP	DIN	DIP		DIN	DIP	DIN	DIP	
1	12.00	0.75	11.52	0.73	12.00N/0.75P	12.00	0.75	12.58	0.47	12.00N/0.75P
2	12.00	0.75	10.97	0.68	12.00N/0.75P	12.00	0.75	12.36	0.51	12.00N/0.75P
3	12.00	0.75	10.63	0.52	12.00N/0.75P	12.00	0.75	12.61	0.51	12.00N/0.75P
4	6.35	1.10	5.65	1.00	6.35N/1.10P	6.35	0.40	6.91	0.18	6.35N/0.40P
5	-	-	-	-	-	17.65	1.10	18.43	0.79	17.65N/1.10P
6	12.00	1.25	10.74	1.14	12.00N/1.25P	20.00	0.75	20.56	0.47	20.00N/0.75P
7	12.00	1.25	11.16	1.12	12.00N/1.25P	20.00	0.75	20.60	0.45	20.00N/0.75P
8	12.00	1.25	10.89	1.09	12.00N/1.25P	20.00	0.75	21.90	0.45	20.00N/0.75P
9	12.00	1.75	10.55	1.56	12.00N/1.75P	4.00	0.75	4.62	0.44	4.00N/0.75P
10	12.00	0.75	10.82	0.61	12.00N/0.75P	17.65	0.40	18.47	0.22	17.65N/0.40P
11	12.00	1.75	10.82	1.58	12.00N/1.75P	4.00	0.75	4.49	0.47	4.00N/0.75P
12	12.00	1.75	11.07	1.53	12.00N/1.75P	4.00	0.75	3.99	0.49	4.00N/0.75P
13	12.00	0.25	11.16	0.14	12.00N/0.25P	2.00	0.75	2.06	0.46	2.00N/0.75P
14	12.00	0.25	11.18	0.16	12.00N/0.25P	6.35	1.10	6.69	0.78	6.35N/1.10P
15	17.65	1.10	16.90	1.01	17.65N/1.10P	2.00	0.75	1.87	0.56	2.00N/0.75P
16	12.00	0.25	11.33	0.15	12.00N/0.25P	2.00	0.75	2.71	0.48	2.00N/0.75P

1028 Table 2. Estimated linear change (per day) ($dS_{275\text{-}295}$) of spectral slope parameters for replicated treatments.

Parameter	Varied P				Varied N			
	12.00N/0.25P	12.00N/0.75P	12.00N/1.25P	12.00N/1.75P	2.00N/0.75P	4.00N/0.75P	12.00N/0.75P	20.00N/0.75P
$dS_{275\text{-}295}$ (nm^{-1} d^{-1})	$-2.3^{x}10^{-3}$	$-3.2^{x}10^{-3}$	$-4.0^{x}10^{-3}$	$-3.0^{x}10^{-3}$	$-1.4^{x}10^{-3}$	$-2.3^{x}10^{-3}$	$-3.2^{x}10^{-3}$	$-3.3^{x}10^{-3}$

Table 3 Spectral characteristics of excitation and emission maximums and range of intensities (Fmax range) of the three fluorescent components identified by PARAFAC modelling in this study and their comparison with previously reported ones

this study				Literature		
Peak (region)	Excitation max	Emission max	Fmax range (RU)	Peak (region)	Autor	Properties
Comp.1	235	440-460 (300)	0.0090-0.0450	1 (<240(355)/476)	Stedmon and Markager 2005	Humic-like; Accumulated in P- and Si- limited bags *Source*: Microbial degradation, *Sink*: Photodegradation
				A (230-260/380-460)	Coble 1996	humic-, fulvik-like; *Sourse*: autochtonous, allochtonous; terrestrial
				C3 (250 (310)/400)	Kowalczuk et al. 2009	*Source*: Bacterial reworking
				C3 (255(330)/412)	Zhang et al. 2009	Terrestrial and marine humic-like; *Source*: microbial activity
				1(<230-260/400-500)	Ishii et al. 2012	Small-sized molecules, Photoresistant, biologically unavailible, conservative tracer; *Source*: Photodegradation
Comp.2	<230(275)	340	0.0200-0.1305	6 (280/338)	Stedmon and Markager 2005	Protein-like; Tryptophan-like fluorescence of protenacious material *Source*: algae at the growth; *Sink*: UV, microbial reworking
				T (275/340)	Coble 2007	Tryptophan-like, protein-like; autochtonous
				peak-T (275/358)	Romera-Castillo et al. 2010	protein-like; *Source*: sterile algae
Comp.3	265	290-300	0.0004-0.2105	4(275/306(338))	Stedmon and Markager 2005	Protein-like: fluorescence of tryptophan and tyrosine in peptides Higher production rates during establishing algal bloom *Source*: growing algae *Sink*: aggregation or microbial uptake
				B (275/305)	Coble 2007	Tyrosine-like, protein-like; *Source*: autochtonous
				C2 (275/<300)	Zhang et al. 2009	Tyrosine-like, protein-like; *Source*: autochtonous
				7 (270/299)	Yamashita et al. 2008	Tyrosine-like, protein-like; *Source*: autochtonous

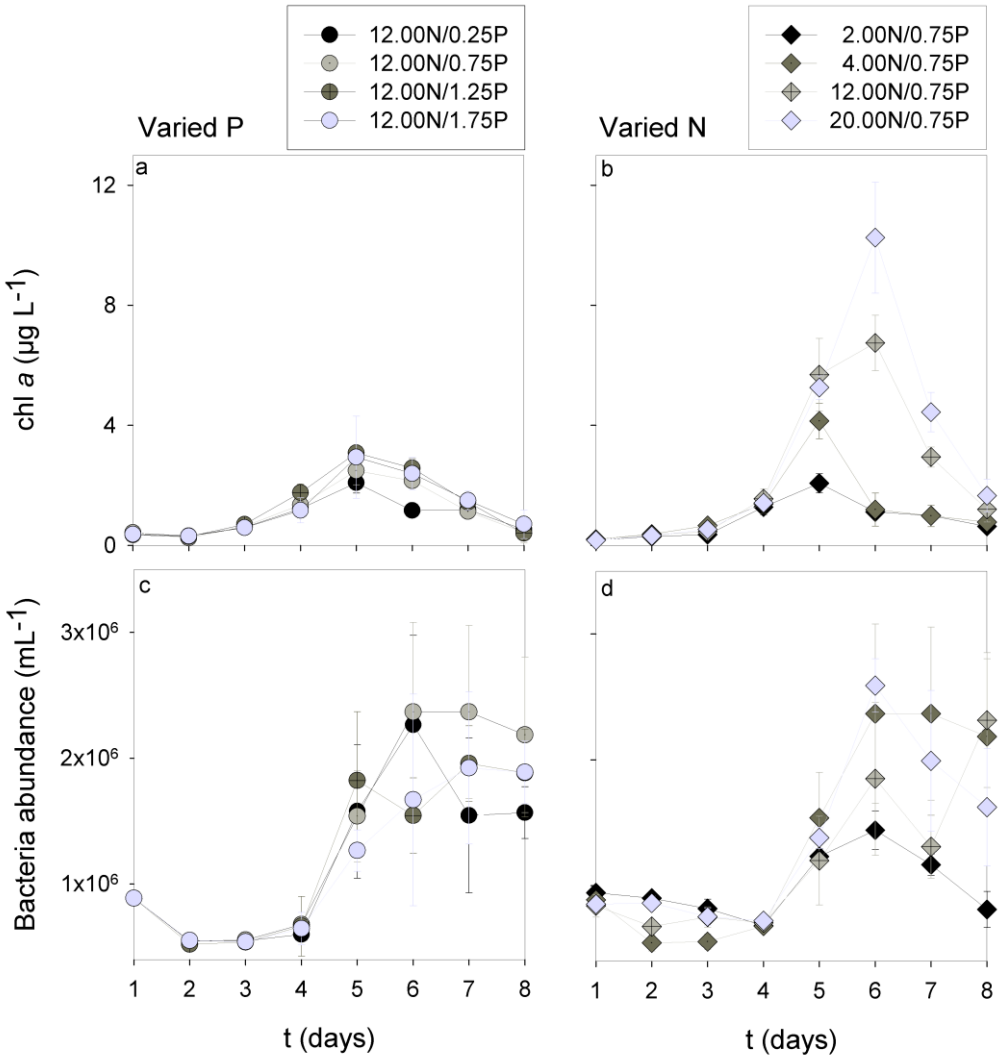

1034

1035 Fig.1 Mean development of chl *a* (a), bacterial abundance (c) in replicated treatments during Varied P;
1036 and chl *a* (b), bacterial abundance (d) in replicated treatments during Varied N

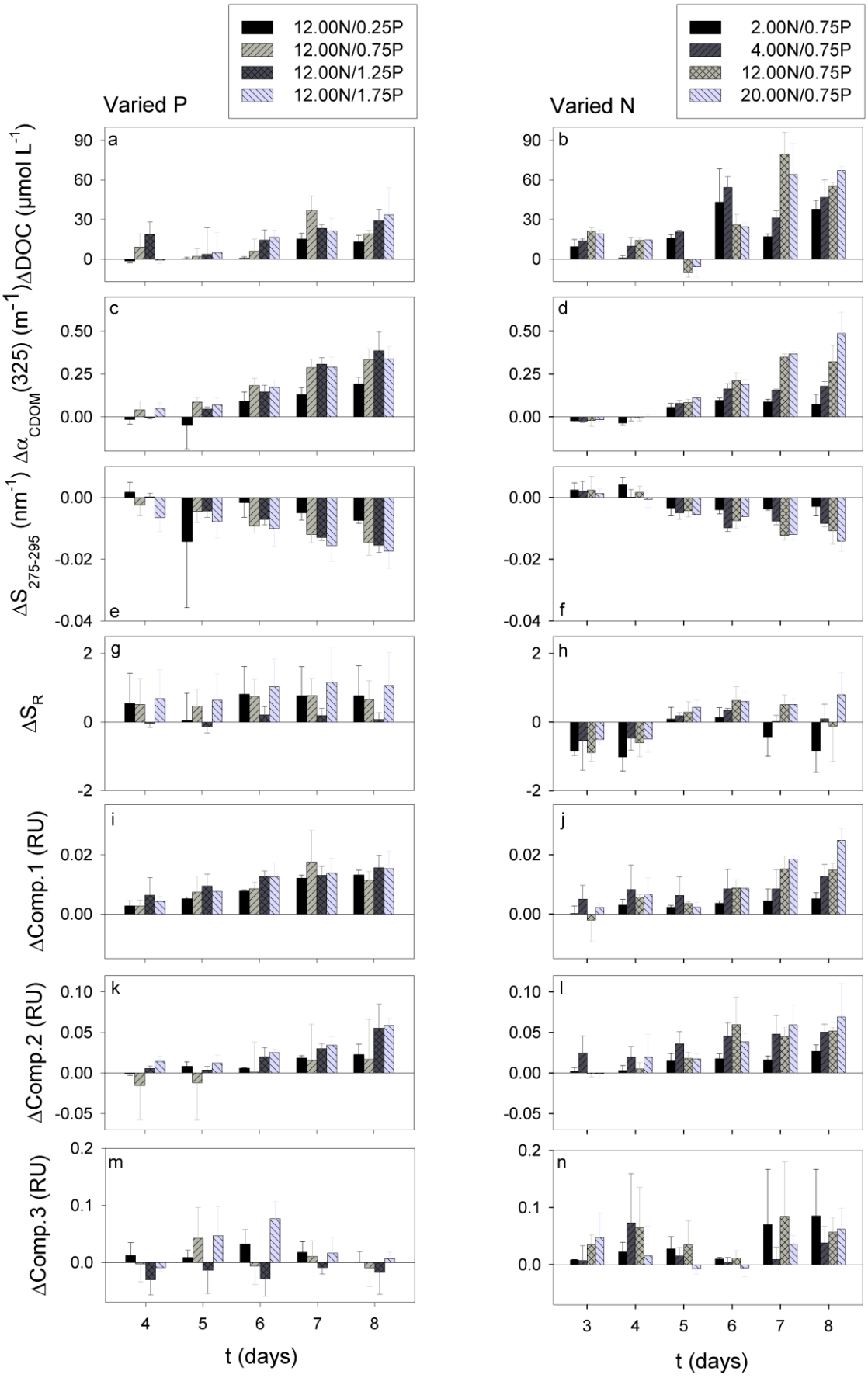

Fig.2 Accumulation over time: of DOC (ΔDOC) (a) during the Varied P and (b) Varied N, of CDOM ($\Delta a_{CDOM}(325)$) (c) during the Varied P and (d) Varied N, of Spectral Slope ($\Delta S_{275\text{-}295}$) (e) during the

Varied P and (f) Varied N, of spectral slope ratio (ΔS_R) (g) during the Varied P and (h) Varied N, of first FDOM component fluorescence intensity (ΔComp.1) (i) during the Varied P and (j) Varied N, of second FDOM component fluorescence intensity (ΔComp.2) (k) during the Varied P and (l) Varied N, of third FDOM component fluorescence intensity (ΔComp.3) (m) during the Varied P and (n) Varied N

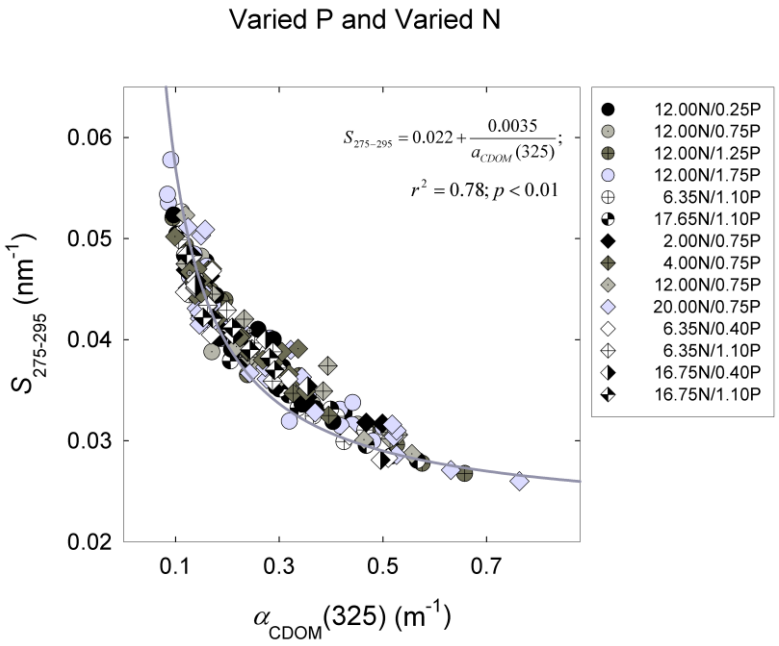

1046

1047 Fig.3 Spectral slope $S_{275\text{-}295}$ against CDOM ($a_{CDOM}(325)$) obtained during both, Varied P and Varied N

1048 experiments (symbols). The dark-grey line is the best fit to the data

1049

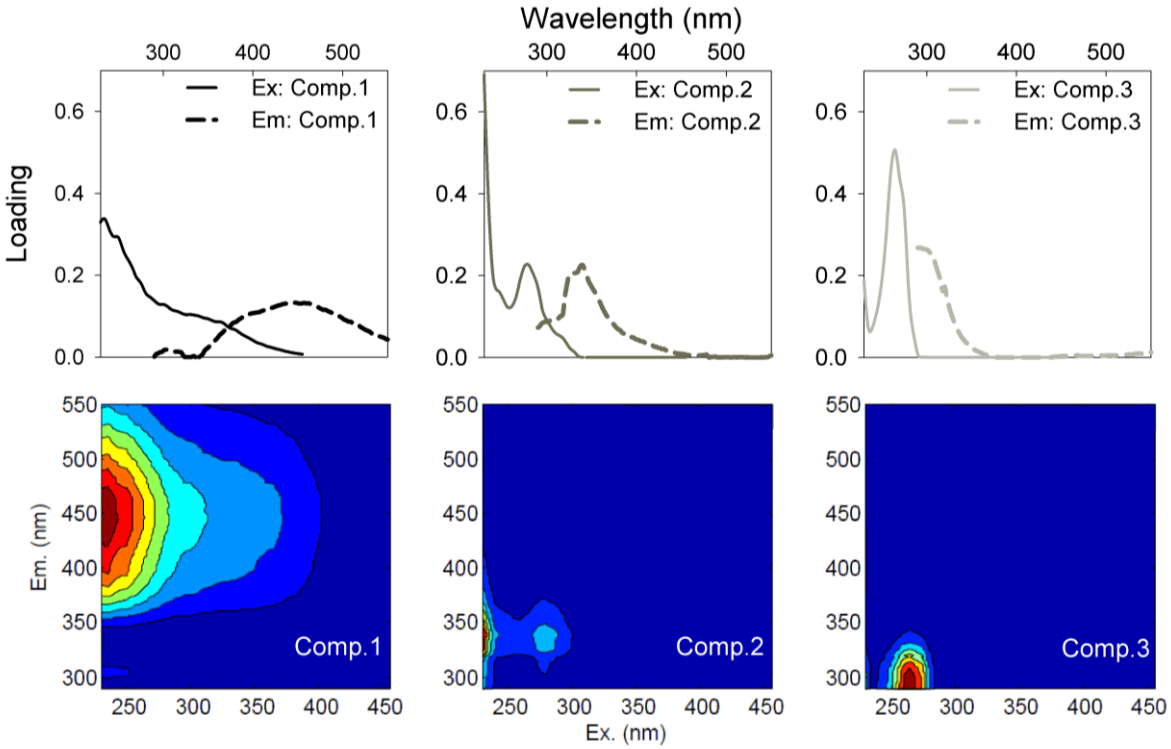

1050

1051 Fig.4. Spectral loadings (upper panel) and fingerprints (lower panel) of the FDOM components

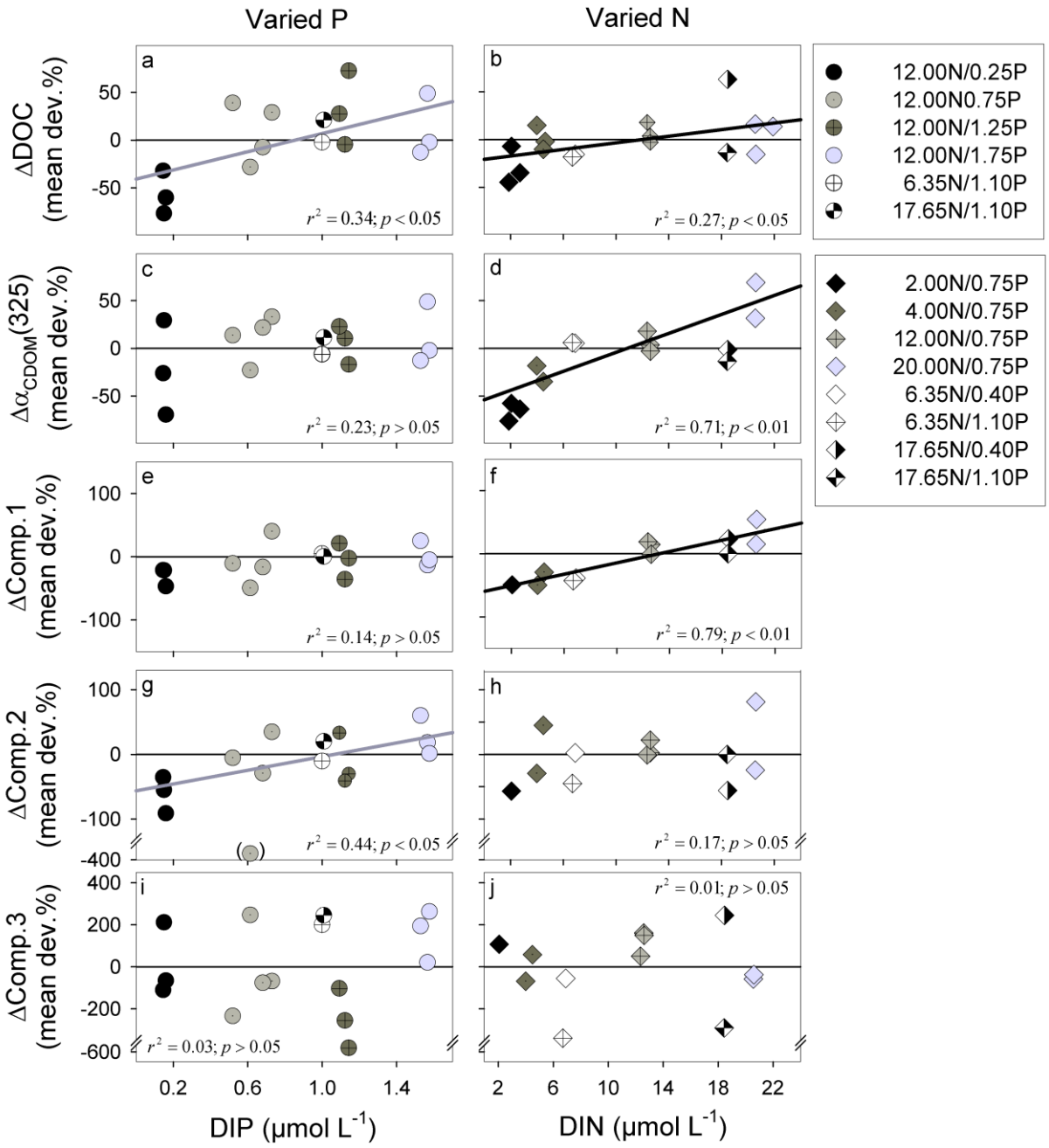

Fig.5. Mean normalized deviations of DOM accumulation against initial nutrients supply. The ΔDOC against DIP initial supply in Varied P (a) and against DIN initial supply in Varied N (b), the CDOM absorption at ($\Delta a_{CDOM}(325)$) against DIP initial supply in Varied P (c) and against DIN initial supply in Varied N (d), the first FDOM component intensity (ΔComp.1) against DIP initial supply in Varied P (e) and against DIN initial supply in Varied N (f), the second FDOM component intensity (ΔComp.2) against DIP initial supply in Varied P (g) and against DIN initial supply in Varied N (h) and the third FDOM component intensity (ΔComp.3) against DIP initial supply in Varied P (i) and against DIN initial supply in Varied N (j) are shown as dashed symbols. The linear regressions are shown by thick light-grey lines in Varied P and by thick black lines in Varied N for those DOM

parameters, where covariance with initial nutrients supply was significant. The symbol in brackets in (g) was considered as an outlier and excluded from linear regression analysis.

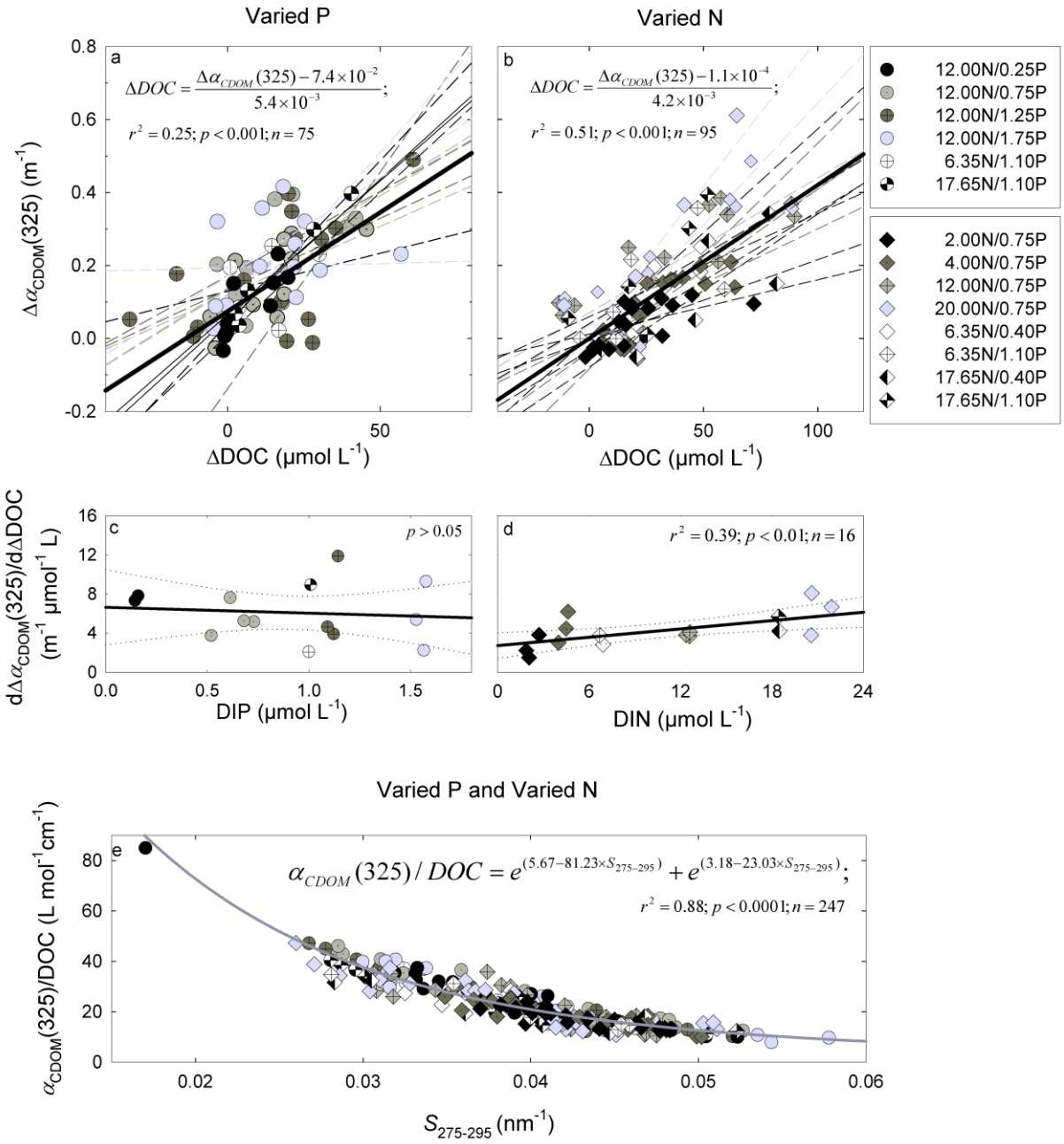

Fig.6 Regression plots of ΔDOC against Δ $a_{CDOM}(325)$ (a) during Varied P (shaded circles) and (b) during Varied N (shaded diamonds). The regression lines for each mesocosm are shown in dashed lines; thick black lines are regressions for all data from Varied P and Varied N respectively. The estimated slopes, of regressions for each mesocosm from (a, b) are plotted as shaded circles for Varied P (c) and shaded diamonds for Varied N. The thick black line is the linear regression line with 95% confidence interval (thin dotted lines). The slope estimated covariance in Varied N to DIN initial supply can be expressed as: $slope\ estimated = 2.7 \times 10^{-3} + 0.14 \times 10^{-3} DIN$ (d). A spectral slope $S_{275\text{-}295}$ against $a_{CDOM}(325)$ /DOC for all mesocosms from both experiments are shown as shaded symbols (e). The dark-grey line is the best fit to the data, obtained in this study.